GEOLOGIC MAP OF THE WISDOM 30' X 60' QUADRANGLE, SOUTHWESTERN MONTANA

Mapped and compiled by:

Colleen Elliott, Jeff Lonn, and Raymond Salazar

Montana Bureau of Mines and Geology

Research supported by the U.S. Geological Survey, National Cooperative Geologic Mapping Program, under USGS award G23AC00457.

Cover Photo: View from Long Peak towards East Goat Peak in the Anaconda Range. The rocks are metamorphosed and overturned Piegan Group sediments in the lower limb of the Fishtrap Nappe. Taken by C. Elliott, MBMG.

GEOLOGIC MAP OF THE WISDOM 30' X 60' QUADRANGLE, SOUTHWESTERN MONTANA

Mapped and compiled by:

Colleen Elliott, Jeff Lonn, and Raymond Salazar

Montana Bureau of Mines and Geology

Montana Bureau of Mines and Geology Geologic Map 106

https://doi.org/10.59691/DOQV3157

August 2025

TABLE OF CONTENTS

FIGURES

TABLE

INTRODUCTION

The Wisdom 30' x 60' quadrangle map is a culmination of detailed and reconnaissance mapping under the USGS STATEMAP component of the National Cooperative Geologic Mapping Program (NCGMP) over a period of 20 yr. Fieldwork was carried out by Montana Bureau of Mines and Geology (MBMG) staff with contributions by members of the Idaho Geological Survey. The quadrangle is in a structurally and stratigraphically challenging area and this map contributes new stratigraphic and structural interpretations as well as many new U-Pb zircon dates.

The map area is mountainous and densely forested. In the western and northern portions of the Wisdom 30' x 60' quadrangle, the Continental Divide, and Continental Divide Hiking Trail, follow the crest of the northern Beaverhead Range and the Anaconda Range. Smooth forested topography of the northern Beaverhead Range transitions northeastward to rugged, high-relief peaks of the Anaconda Pintler Wilderness. The Pioneer Mountains on the east also have rounded forested topography and up to 1,200 m (4,000 ft) of relief. The Big Hole River transecting the map is the westernmost headwaters of the Missouri River. The broad, sparsely populated Big Hole River Valley is dominated by ranch land and hay fields. In the northwest corner of the quadrangle, the headwaters of the Columbia River system are represented by the East Fork of the Bitterroot River.

Only three paved roads and a scattering of gravel roads serve the map area. The Anaconda Pintler Wilderness and West Pioneer Wilderness Study area are roadless and can only be accessed on foot. Since 2000, wildfires have burned at least half of the uplands in the quadrangle, making passage very difficult.

PREVIOUS WORK

Figure 1 shows the footprints of previous geologic maps of the Wisdom 30' x 60' quadrangle. Prior to STATEMAP Program mapping, a large part of the quadrangle had only been covered at 1:250,000 scale (Ruppel and others, 1993), with 1:50,000 scale coverage of the Anaconda Pintler Wilderness (Wallace and others, 1992), part of the Pioneer Range (Berger and others, 1983a,b), and the northwest corner of the quadrangle (Desmarais, 1983). The Wisdom 30' x 60' geologic map relies heavily on the Desmarais (1983) map for coverage of an area that now has difficult access and copious deadfall.

STRATIGRAPHY

Proterozoic Stratigraphy

Extensive exposures of the Mesoproterozoic Belt Supergroup underlie the mountains of the Wisdom

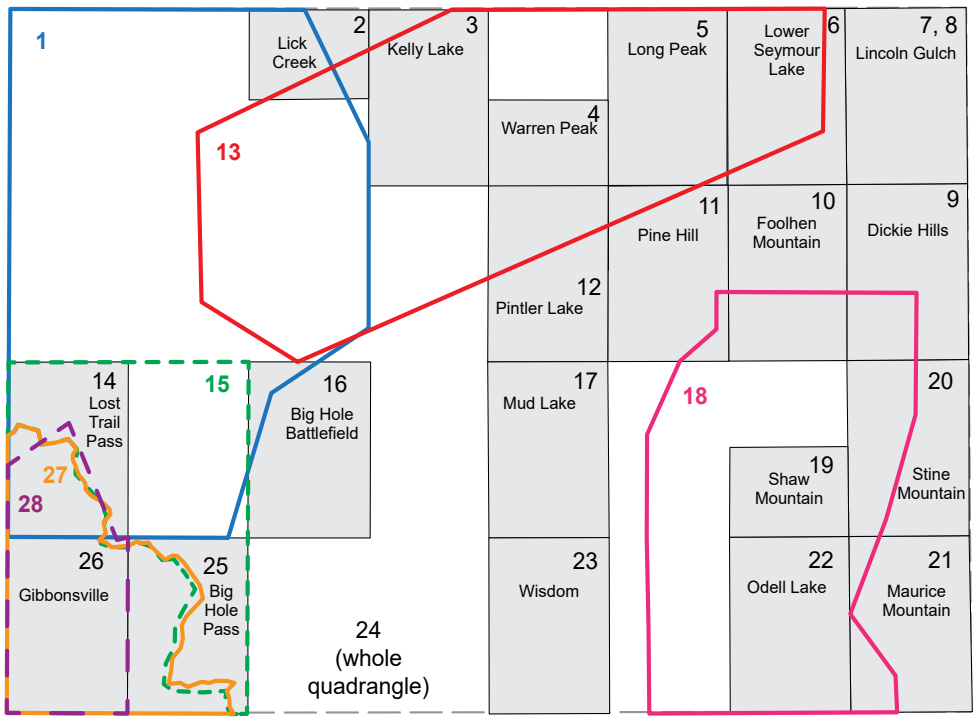

1 Desmarais, 1983 1:50,000
2 Lonn, 2017 1:24,000
3 Lonn and McDonald, 2004 1:24,000
4 Howlett and others, 2020 1:24,000
5 Elliott and Lonn, in prep 1:24,000
6 Elliott, 2015 1:24,000
7 Elliott, 2017 1:24,000
8 Lewis, 1993 1:24,000
9 Lonn and McDonald, 2004 1:24,000
10 Elliott and Lonn, 2021 1:24,000
11 Hanneman, 1987b; Elliott, 2022 1:24,000
12 Hanneman, 1987a 1:24,000
13 Wallace and others, 1992 1:50,000
14 Stewart and others, 2025 1:24,000
15 Lopez and others, 2005 1:48,000
16 Elliott, 2024 1:24,000
17 Hanneman, 1984 1:24,000
18 Berger and others, 1983 1:50,000
19 Lonn, 2020 1:24,000
20 Lonn and Elliott, 2017 1:24,000
21 Lonn, 2015 1:24,000
22 Lonn and Scarberry, 2022 1:24,000
23 Hanneman, 1984 1:24,000
24 Ruppel and others, 1993 1:250,000
25 Lonn and others, 2024 1:24,000
26 Lopez, 1982 1:24,000
27 Evans and Green, 2003 1:100,000
28 Stewart and others, 2014 1:40,000

Figure 1. Previous mapping, Wisdom 30’ x 60’ quadrangle.

quadrangle. The Belt Supergroup is an immensely thick (as much as 15 km (9.3 mi)) sedimentary succession deposited in a vast intracratonic basin from about 1.47 to 1.38 Ga (Lonn and others, 2020). In the north-central part of the map, in the footwall of the Anaconda Detachment Zone (ADZ) and Georgetown thrust, the strata represent the entire Belt stratigraphic section, although it has been tectonically thinned (see Structure and Tectonics section). The rest of the quadrangle exposes Lemhi subbasin strata correlative with the Missoula Group of the upper Belt Supergroup. Lemhi subbasin strata are also very thick (>14 km, 8.6 mi), but are much sandier, with a dissimilar stratigraphic sequence (Burmester and others, 2016). The Lemhi strata are interpreted to be the southern, upstream ends of huge alluvial aprons that fed the Belt inland sea during Missoula Group (upper Belt) time (Lonn and others, 2023). Lemhi nomenclature (Burmester and others, 2016) is used on most of the map, while standard Belt Formation names (Lonn and others, 2020) are used in the north-central part. For information on specific formation correlations, see the correlation chart.

The eastern margin of the Belt Basin is present along the eastern edge of the map, although it is obscured by the Cretaceous–Tertiary Maurice Mountain thrust and Fourth of July normal fault (fig. 2). West of these faults is a thick (>5,000 m, >16,000 ft) section of Lemhi strata; east of the faults, only a very thin (500 m, 1,600 ft) Belt section is present, consisting solely of the Black Lion Formation. The conglomeratic Black Lion Formation is thought to be a coarse-grained, basin-marginal facies deposited unconformably on the Paleoproterozoic basement along the steep eastern shore of the Belt Sea (McDonald and others, 2012). It is postulated to interfinger with the Lemhi strata to the west (McDonald and Lonn, 2013), but is now separated from them by the Maurice Mountain thrust and Fourth of July faults. Similarly, the contacts between the Lemhi subbasin strata and the more typical Belt Basin units in the northern part of the quadrangle are

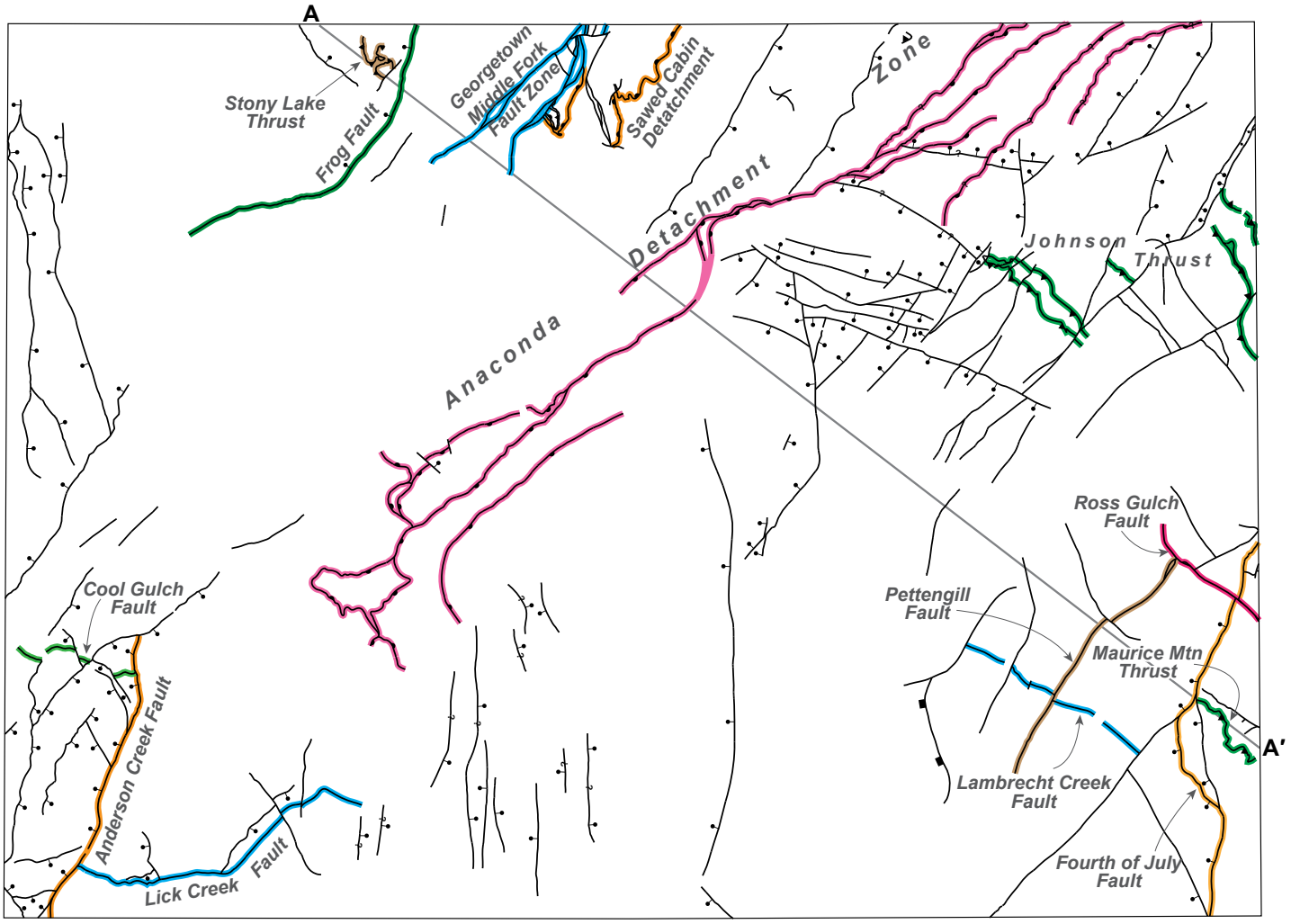

Figure 2. Fault map with cross-section location. Named fault zones are colored to show their extent.

faults, and therefore facies relationships are concealed. See Lonn and others (2023) for more detail on correlations between the two.

Paleozoic and Mesozoic Stratigraphy

Paleozoic and Mesozoic sedimentary and metasedimentary rocks occur in small areas near the eastern border of the Wisdom 30' x 60' quadrangle. Cambrian metasedimentary rocks also occur in a small area in the north-central part of the quadrangle where they have been tectonically thinned in the footwall of the ADZ (see section below discussing footwall folds and fabrics). Cretaceous metamorphic rocks with Carboniferous through Cretaceous sedimentary protoliths (unit KMsm) are part of the Foolhen Complex described below in the intrusive and metamorphic rocks section.

Cenozoic Stratigraphy

Cenozoic strata within the Wisdom quadrangle are stratigraphically continuous with those of the Deer Lodge basin in the northeast-adjacent Butte North 30' x 60' quadrangle (Scarberry and others, 2019) and the south-adjacent Salmon 30' x 60' quadrangle (Lonn and others, 2019). The Cenozoic sediments and sedimentary rocks belong to the Bozeman Group, which is here considered to include strata deposited from Paleogene through Neogene, before glaciation, and include the Challis–Lowland Creek Volcanic Complex and the Renova and Sixmile Creek Formations.

Challis–Lowland Creek Volcanic Complex

The Challis–Lowland Creek Volcanic Complex (CLCV) described here combines the Challis Volcanic Group in Idaho and the Lowland Creek volcanic field in Montana. The CLCV includes sedimentary as well as extrusive and intrusive components. In the Wisdom 30' x 60' quadrangle, the Lowland Creek Volcanic complex transitions into the Challis Volcanic Group with no apparent distinction in composition or age between the two.

The Challis Volcanic Group, though not well dated in Idaho, is generally thought to range between about 52 and 46 Ma (Mosolf and others, 2023a,c; Mosolf and Kylander-Clark, 2023a; Brennan and others, 2025). The Challis Group is part of the much larger Kamloops–Challis–Absaroka belt (Armstrong and Ward, 1991) which, taking into account modern geochronologic data, has an age range between ca. 57 and 45 Ma (Dostal and Jutras, 2022; Mosolf and others, 2023b; Mosolf and Kylander-Clark, 2023a; Van Wagoner and Ootes, 2024; Brennan and others, 2025). The Challis Volcanic Group discussed here correlates with the Challis intrusive suite described by Gaschnig and others (2011), who report a range in age between approximately 51 and 44 Ma.

In the Wisdom quadrangle, CLCV ages range between 52 and 49 Ma (AH21WW4, 23RB430, table 1) for rhyolitic and dacitic volcanic and hypabyssal rocks. In the northeast-adjacent Butte North quadrangle, Lowland Creek ages range between 53 and 48 Ma (Dudas and others, 2010).

The CLCV includes abundant clastic sedimentary interlayers. The oldest Cenozoic sedimentary rocks within the Wisdom quadrangle are volcanogenic siliciclastic rocks (map unit Tvs) near Big Hole Battlefield in the south-central part of the map, which have a maximum depositional age (MDA) of ca. 64.5 Ma (CE20BHB8, table 1) and appear to rest directly on granitoid rocks map unit Tbmg, which is dated 63.3 ± 0.6 Ma (CE20BHB15, table 1). This gives the unit an MDA of 63.3 Ma. A rare ash layer in the Tvs package near Big Hole Battlefield yielded a U-Pb zircon age of 51.4 ± 1 Ma (CE20BHB02, table 1), which is probably a more reasonable age for the unit.

Map relationships and U-Pb zircon data show that CLCV rocks were erupted onto and within early Eocene fluvial/alluvial sediments in the deeply incised ancestral Big Hole, Bitterroot, and Salmon River Valleys (Schwartz and others, in review). At Big Hole Battlefield the sedimentary and volcanic package is over 600 m (2,000 ft) thick.

The Eocene East Fork Dike Swarm (map units Tds and Tdsr; Hyndman and others, 1977; Bausch, 2013) occupies a large part of the west side of the map. The swarm includes a large area where dikes and sills are too dense to separate, as well as scattered dikes and sills that extend from it. The East Fork Dike Swarm is genetically related to the volcanic complex (Bausch and others, 2013; Stewart and others, 2025), with U-Pb zircon ages ranging from 51.2 ± 0.4 to 52.7 ± 0.3 (AH21WW8, 23RL043, table 1). At Saddle Mountain, the dike swarm is overlain by extrusive rhyolitic flows with a U-Pb zircon age of 49.3 ± 0.2 Ma (23DS19, table 1). Bausch (2013) and Bausch and others (2013) report $^{40}Ar/^{39}Ar$ biotite cooling ages of

Table 1. U-Pb zircon ages for the Wisdom quadrangle.

Sample	Rock Type and Location	Unit	Latitide (ºN)	Longitutde (ºW)	Method	No. of Spot Analyses[a]	Age (Ma)	2σ	Reference(s)
CE23W100K10	Sand from quarry in the Rock Creek drainage, south Big Hole Valley	Tsc	45.5515	-113.5384	MDA 206/238	120	10.8	0.4	ADYY Brennan
23RDS11	Pine Hill basalt	Tba	45.8603	-113.2810	WM 206/238	40	25.3	0.6	ADYY Brennan
23RDS09	Pine Hill basalt	Tba	45.8638	-113.3451	WM 206/238	117	25.6	0.4	ADYY Brennan
CE22BHB01	Matrix of two-mica sandstone near big Hole Battlefield	Tre	45.6379	-113.6560	MDA 206/238	183	26.2	0.4	AD5
CE21WE02	Ash bed near Pintler Lake	Tre	45.8112	-113.4140	WM 206/238	40	26.4	0.1	AD4
CE19PH5	Ashy silt bed near Mud Creek	Tre	45.8658	-113.3821	MDA 206/238	140	31.7	0.8	ADXX Mosolf
23RB430	Rhyolite tuff, North Fork Salmon River	Tcv	45.5465	-113.9810	WM 206/238	40	49.0	0.2	ADYY Brennan
23DS19	Rhyolite phase of Saddle Mountain volcanic field	Tr	45.7188	-113.9910	WM 206/238	40	49.3	0.2	ADYY Brennan
AH21WW3	Large dike at Lost Trail Pass	Tqs	45.6989	-113.9748	WM 206/238	40	49.3	0.2	AD4; AD1
AH21WW8	Rhyolite dike at West Fork Camp Creek	Tdsr	45.7417	-113.9523	WM 206/238	38	51.2	0.4	AD4; AD1
CE20BHB02	Ash layer from Battle Mountain	Tvs	45.6698	-113.6844	WM 206/238	40	51.4	1.0	AD3
CE20BHB18	Sand bed from roadcut west of Wisdom	Tsc	45.6301	-113.5280	MDA 206/238	40	51.5	0.6	AD3
CE20BP5	Dacite dike near Mussigbrod Lake	TKYhcs	45.8069	-113.6379	WM 206/238	40	51.7	0.8	AD3
CE20BHB17	Sand interlayered with cemented conglomerate near Big Hole	Tre	45.6379	-113.6561	MDA 206/238	40	51.9	0.6	AD3
AH21WW4	Volcanic complex at Saddle Mountain	Tbdt	45.7115	-113.9952	WM 206/238	39	52.2	0.4	AD4; AD1
23RDS10	Pine Hill basalt	Tba	45.8622	-113.2825	MDA 206/238	40	52.4	0.3	ADYY Brennan
AH21WW5	Dacite dike near East Fork Camp Creek	Tds	45.7156	-113.9192	WM 206/238	40	52.4	0.2	AD4; AD1
23RL043	Dacite dike near Lost Trail Pass	Tdsr	45.6788	-113.9637	WM 206/238	40	52.7	0.3	ADYY Brennan
CE20BP3	Unfoliated biotite ± muscovite granite near Mussigbrod Lake	TKhcs	45.8069	-113.6379	WM 206/238	40	61.6	0.5	AD3
AH21WW12	Burnt Ridge Pluton near Sula	Tgbm	45.8358	-113.9855	WM 206/238	40	62.8	0.6	AD4; AD1
CE19PH11a	Intrusion within Foolhen Pluton	Tgbm	45.7664	-113.2499	WM 206/238	40	62.8	1.0	Elliott, 2022; ADYY Brennan
CE18BP1	Nonfoliated biotite granite Mussigbrod Lake	TKhcs	45.8070	-113.6450	WM 206/238	39	63.3	0.6	This report
CE20BHB15	Trail Creek Pluton	Tgbm	45.6519	-113.7086	WM 206/238	40	63.3	0.6	AD3
CE20BP4	Aplite dike near Mussigbrod Lake	TKYhcs	45.8069	-113.6379	WM 206/238	40	63.3	0.7	AD3
AH21WW10	Rye Creek Pluton	Tgbm	45.9930	-113.9348	WM 206/238	38	64.4	0.8	AD4; AD1
CE20BHB8	Volcanogenic siltstone and sandstone near Johnson Creek	Tvs	45.7268	-113.6531	WM 206/238	40	64.5	1.2	AD3
CE19PH7	Doolittle Pluton	KTg	45.7516	-113.3668	WM 206/238	39	68.2	0.8	Elliott, 2022; ADXX Mosolf
KCS2110	Uphill Creek Pluton	Kgdp	45.5226	-113.0548	WM 206/238	40	68.2	0.3	AD4; AD1
CE19PH1	Proposal Rock Pluton	Kgd	45.6257	-113.3293	WM 206/238	40	68.4	0.5	Elliott, 2022
KCS2004	Odell Lake Plulton	Kgdb	45.5752	-113.2352	WM 206/238		68.7	0.5	Lonn and Scarberry, 2022
KCS2019	Mono Park Pluton	Kgdf	45.5119	-113.1799	WM 206/238		70.1	0.4	Lonn and Scarberry, 2022
KCS2129	Uphill Creek Pluton	Kgdp	45.5084	-113.0403	WM 206/238	39	70.7	0.5	AD4; AD1
KCS2130	Uphill Creek Pluton	Kgdp	45.5095	-113.0386	WM 206/238	39	70.9	0.4	AD4; AD1
KCS2012	Stewart Mountain Pluton	Kgdf	45.5239	-113.2118	WM 206/238		71.8	0.5	Lonn and Scarberry, 2022
AH21WW9	Martin Creek Pluton	Kgdf	45.9093	-113.8478	WM 206/238	40	72.3	0.4	AD4; AD1
CE19FH1	Foolhen Pluton	Kgdf	45.8100	-113.1642	WM 206/238	40	72.5	0.5	ADXX Mosolf
KCS2134	Biotite granite sill in Yq adjacent to the Francis Creek Pluton	Kg	45.5400	-113.3565	WM 206/238	39	72.9	0.4	AD4; AD1
CE16FH1[b]	Migmatite gneiss within the Foolhen Complex	Yqsg	45.8572	-113.2452	single grain[c]	1	73.0	2.0	Elliott and Lonn, 2021
CE18FH9[b]	Migmatite gneiss within the Foolhen Complex	Yqsg	45.8170	-113.1681	single grain[c]	1	73.1	2.3	Elliott and Lonn, 2021
CE18FH13a	Foolhen Complex	Kgn	45.7899	-113.1469	WM 206/238	53	73.3	0.4	Elliott and Lonn, 2021

Table 1—*Continued*.

KCS2136	Francis Creek Pluton	Kg	45.5483	-113.3631	WM 206/238	38	73.3	0.6	AD4; AD1		
KCS2112	Foolhen Complex	Kgdf	45.6494	-113.1800	WM 206/238	40	73.7	0.3	AD4; AD1		
CE18FH14	Foolhen Complex	Kgd	45.7869	-113.1901	WM 206/238	44	73.9	0.4	Elliott and Lonn, 2021		
KCS2111	Stine Creek Pluton	Kg	45.7239	-113.0363	WM 206/238	38	74.6	0.8	AD4; AD1		
CE23W100K08	Dodgson Creek Pluton	Kgd	45.8825	-113.0014	WM 206/238	40	76.1	0.3	ADYY Brennan		
CE20BP2	Orthogneiss near Mussigbrod Lake	TKhcs	45.8069	-113.6379	WM 206/238	40	76.3	0.3	AD3		
CE20BP1	Foliated biotite granitoid near Mussigbrod Lake	TKhcs	45.8069	-113.6379	WM 206/238	40	76.5	0.6	AD3		
23RL030	Kgdf sheet within complex near Lost Trail Pass	TKhcs	45.6723	-113.9532	WM 206/238	40	76.8	0.4	ADYY Brennan		
23RB406	Anderson Creek Mafic Dike	Yim	45.6202	-113.8930	WM 206/238	9	1264	15	AD16 Brennan		
CE19PH4	Metasediments near Big Hole River and Chalk Bluff	Yqsg	45.8119	-113.3084	WM 206/238	100	1715	6.3	ADXX Mosolf		

Note. Reported ages are the weighted mean of the ^{207}Pb corrected ^{206}Pb/^{238}U ages obtained for each sample. Method: WM 206/238 weighted mean of select ^{206}Pb/^{238}U dates. Includes ages previously published with MBMG Geologic Maps as well as ages published in MBMG Analytical Datasets: AD3, Mosolf and Kylander-Clark (2023a); AD4, Mosolf and Kylander-Clark (2023b); AD5, Mosolf and others (2023a); AD16, Brennan and others (2025); ADXX, Mosolf and others (in review). Geochemical data are reported in AD1, Mosolf and others (2023b). Zircon separates were prepared at the MBMG and analyzed by LA-ICPMS at the University of California, Santa Barbara, CA. Latitudes and longitudes are in the 1984 World Geodetic Survey (WGS84) datum. MDA 206/238, max depositional age, weighted mean of youngest ^{206}Pb/^{238}U dates. MEA 207/206, maximum emplacement age, weighted mean of oldest overlapping ^{207}Pb/^{206}Pb dates.

[a]Number of spot analyses used to calculate weighted mean age.
[b]Zircon spectra shown in Elliott and Lonn (2021).
[c]Concordant igneous zircon has a Cretaceous age. Inherited zircon spectrum has Belt Supergroup affinities.

approximately 52–48 Ma. Within the >10-km (>6-mi) swath of Tds and Tdsr, there is no mappable country rock, suggesting accommodation of at least 10 km (6 mi) of extension during dike emplacement.

Granitoid intrusions in the Anaconda Range outside the Wisdom 30' x 60' quadrangle have ^{40}Ar/^{39}Ar ages that overlap with the CLCV (Wallace and others, 1992; Foster and others, 2010) Neal and others (2023a,b) obtained a U-Pb zircon age for the Beaverhead Mountain Pluton just north of the Wisdom quadrangle.

Challis and Lowland Creek volcanic rocks are commonly considered to be related to a volcanic arc, but the absence of a proximal subduction zone suggests otherwise. The Challis and Lowland volcanic rocks are the same age as regional extension and are spatially and temporally related to hypabyssal rocks that form the East Fork Dike Swarm, which accommodates extension beyond the southern end of the ADZ. Busby and others (2023) and references therein suggest that the widespread Eocene volcanic rocks in the northwest United States and southern British Columbia are related to a regional pull-apart system driven by dextral transtension.

Renova and Sixmile Creek Formations

U-Pb zircon data and sparse fossil data along with detailed mapping allow distinction between Renova (Tre) and Sixmile Creek (Tsc) equivalent strata (summarized by Vuke, 2019) in some parts of the Wisdom quadrangle, but not all. Areas where the distinction is unclear are mapped as Ts where fine-grained sediments are present or Tgr for gravel deposits. Along the east side of the Big Hole Valley, the unconformity between Tre and Tsc is well exposed. Roe (2010) reports that the sediments below the unconformity contain fossils identified as Arakareean (approximately 29–20 Ma) and sediments above the unconformity contain fossils tentatively identified as Barstovian (approximately 16–13 Ma). In the north-central part of the Big Hole Valley, ashy clastic sediments are separated from gravels by the Pine Hill basalt (Tba), which yielded a U-Pb zircon MDA of 25.6 ± 0.3 Ma (weighted mean from samples 23RDS09, 23RDS10, and 23RDS11combined, table 1). South of Pine Hill near Pintler Creek, an ash bed in Tre below a well-exposed angular unconformity with a thick paleosol has a U-Pb zircon age of 26.4 ± 0.1 Ma (CE21WE02,

table 1). Thick fluvial Tsc sand and gravel overlies the unconformity, and in the middle of the valley near the south edge of the Wisdom quadrangle has an MDA of 10.8 ± 0.4 Ma (CE23W100k-10, table 1). In other places where Tre and Tsc are distinguished, they are separated by an angular unconformity between underlying sediment with ashy beds and overlying fluvial cobble gravel, at the same stratigraphic level as the Pine Hill basalt.

Provenance analyses of Renova-aged sediments in the Big Hole and adjacent river valleys demonstrate that currently existing highlands were being eroded and shedding sediments into incised valleys by 52 Ma (Schwartz and others, in prep.). Drill hole and geophysical evidence summarized by Roe (2010) reveal that Tre in the Pine Hill area is over 2,000 m (6,600 ft) thick. Just south of the south edge of the Wisdom quadrangle (Roe's transect B–B'), the Big Hole basin is 2,464 m (8,084 ft) deep, though the individual thicknesses of Tvs, Tre, and Tsc are unknown.

INTRUSIVE AND METAMORPHIC ROCKS

The west side of the Wisdom quadrangle is dominated by the Chief Joseph Plutonic–Metamorphic Complex of Desmarais (1983), herein referred to as the Chief Joseph Complex (fig. 3). The Chief Joseph Complex is at the easternmost extent of the Idaho Batholith. Based on Desmarais (1983) and new U-Pb zircon dating from this project (table 1), the Chief Joseph Complex can be divided into the following components:

1. Sillimanite-bearing, metamorphic to migmatitic, Belt-aged xenoliths (Yqsg, Yqcs) within and along the edges of the plutonic phases,
2. Gneissic to nonfoliated biotite ± hornblende-bearing granite and granodiorite (Kg, Kgdf, approximately 77–72 Ma),
3. Paleogene biotite ± muscovite-bearing granitoids (Tgbm, approximately 65–60 Ma), and
4. CLCV-related hypabyssal rocks (approximately 53–47 Ma).

Where all of these components are too closely interlayered to map separately, they are portrayed as the Hell Roaring Creek Subcomplex (unit TKYhcs on map).

On the east side of the Wisdom quadrangle, the Foolhen Complex dominates the West Pioneer Mountains. The Foolhen Complex has similar components:

1. Sillimanite-bearing, metamorphic to migmatitic, Belt-aged rocks (Yqsg),
2. Gneissic to nonfoliated biotite ± hornblende-bearing granodiorite (Kgdf, approximately 72–74 Ma),
3. Gneiss of Foolhen Ridge (Kgn, approximately 73 Ma),
4. Paleogene biotite ± muscovite-bearing granitoids (Tgbm, approximately 68–63 Ma), and
5. Cretaceous metamorphic rocks with Carboniferous through Cretaceous sedimentary protoliths (KMsm).

CLVC-related rocks were not observed in the West Pioneer Mountains.

In both complexes, peak metamorphism occurred at the same time as Cretaceous plutonism, and was syntectonic (Desmarais, 1983; Elliott and Lonn, 2021; Elliott, 2022).

TECTONIC HISTORY

Summary

The tectonic history and structural geology of the Wisdom quadrangle are challenging. The earliest recognized structures are Mesoproterozoic growth faults that must have controlled the steep eastern Belt Basin margin and were undoubtedly active within the basin (McDonald and others, 2012; Lonn and others, 2023). In Cretaceous through Paleocene times, interference folds and significant reverse faults like the Stony Lake, Georgetown, and Maurice Mountain thrusts formed in response to Cordilleran shortening. By late Paleocene times, the plutonic–metamorphic complexes bordering the Big Hole Valley were exposed and shedding detritus into the proto-Big Hole Valley. Cordilleran contraction was followed by low-angle extension on the ADZ starting ca. 53 Ma (Foster and others, 2010). High-angle normal faults within the Big Hole Valley reactivated some older structures and remained active through the late Miocene.

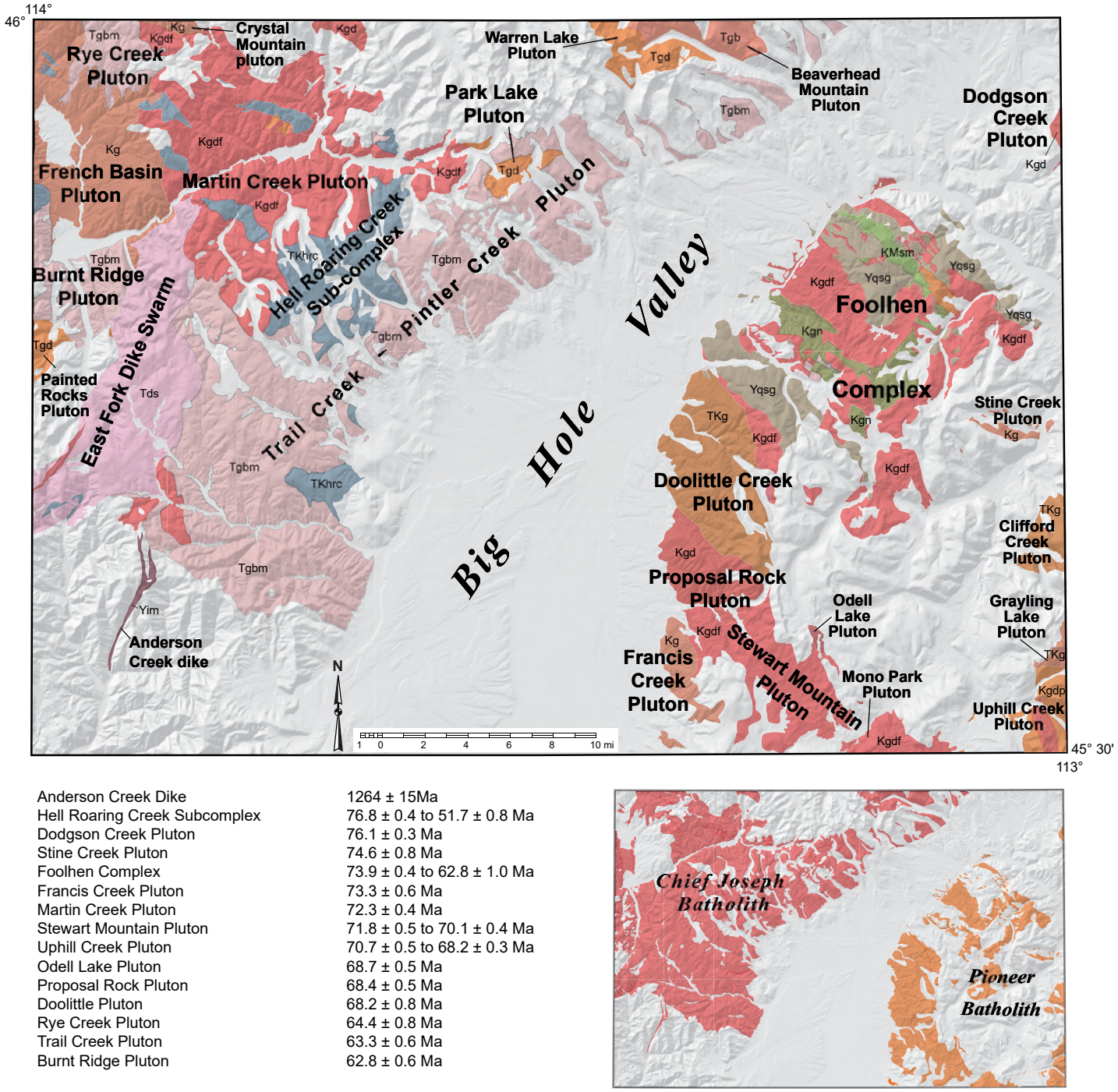

Anderson Creek Dike	1264 ± 15Ma
Hell Roaring Creek Subcomplex	76.8 ± 0.4 to 51.7 ± 0.8 Ma
Dodgson Creek Pluton	76.1 ± 0.3 Ma
Stine Creek Pluton	74.6 ± 0.8 Ma
Foolhen Complex	73.9 ± 0.4 to 62.8 ± 1.0 Ma
Francis Creek Pluton	73.3 ± 0.6 Ma
Martin Creek Pluton	72.3 ± 0.4 Ma
Stewart Mountain Pluton	71.8 ± 0.5 to 70.1 ± 0.4 Ma
Uphill Creek Pluton	70.7 ± 0.5 to 68.2 ± 0.3 Ma
Odell Lake Pluton	68.7 ± 0.5 Ma
Proposal Rock Pluton	68.4 ± 0.5 Ma
Doolittle Pluton	68.2 ± 0.8 Ma
Rye Creek Pluton	64.4 ± 0.8 Ma
Trail Creek Pluton	63.3 ± 0.6 Ma
Burnt Ridge Pluton	62.8 ± 0.6 Ma

Figure 3. Names, U-Pb zircon ages, and locations of plutons in the Wisdom 30' x 60' quadrangle. See table 1 for sources of age data.

Major tectonic features and structures of the quadrangle are described individually below. Faults named in the text are shown in figure 2.

Precambrian Faults

The Fourth of July fault along the east side of the Wisdom quadrangle was a growth fault during the deposition of Belt Supergroup sediments in Mesoproterozoic times and was reactivated in the Tertiary. It separates blocks with distinct stratigraphic sections: over 2,000 m (6,600 ft) of Lemhi Subbasin strata on the west, downthrown, side, and a much thinner 500 m (1,600 ft) Belt section on the east side, consisting of the Black Lion Formation that is interpreted to be coarse marginal facies of the eastern edge of the Belt Basin.

Several other faults in the Wisdom quadrangle have been intruded by Precambrian dikes. In the southeastern corner of the map, a diorite dike (ZYdi)

with a whole-rock $^{40}Ar/^{39}Ar$ minimum age of 660 Ma (Zen, 1988) intrudes along the west–northwest-striking Lambrecht Creek fault, making the fault Neoproterozoic or older. The sense of movement on the Lambrecht Creek fault is uncertain, although stratigraphic relations suggest southside-down offset.

Two east–west-striking faults in the southwest corner of the quadrangle—the Lick Creek (Stewart and others, 2014) and Cool Gulch (Stewart and others, 2025) faults—juxtapose Yqcs and Ysw or Yg, whose stratigraphic relationships are unknown. The faults' dips and sense of movement remain uncertain. The two faults were postulated to be a single fault offset by a younger cross-fault, the Anderson Creek fault, (Stewart and others, 2014). A mafic intrusion (Yim) intruded along the Anderson Creek fault has a U-Pb zircon crystallization age of 1,264 ± 15 Ma (23RB406, table 1). Therefore, if the Cool Gulch and Lick Creek faults were originally contiguous but later offset by the Anderson Creek fault, they were active in the Proterozoic. The Cool Gulch fault is also truncated by Tertiary intrusive rocks (Tds).

Cretaceous Thrust Faults

Segments of regional-scale thrust faults are present in the Wisdom quadrangle. The Stony Lake thrust and the structurally lower Georgetown–Philipsburg thrust are exposed in the north-central part of the map. The Stony Lake thrust places Piegan Group strata over younger Lemhi strata (Lonn and Mosolf, 2020) and is well exposed in the northwestern part of the quadrangle along Moose Creek and Sign Creek (see Lonn, 2017, for details). The east-directed Georgetown–Philipsburg thrust system brings Piegan Group rocks over younger Missoula Group and Paleozoic strata, and over Mesozoic strata on the north-adjacent Philipsburg 30' x 60' quadrangle (Lonn and others, 2003). The original Georgetown–Philipsburg thrust geometries are not, however, preserved in the Wisdom quadrangle. The thrusts have been cut by high-angle faults of the northeast-striking Georgetown Middle Fork fault (Lonn and McDonald, 2004a) that now separates the Georgetown–Philipsburg thrust's hanging wall and footwall. The hanging wall and footwall carry different Belt sections. The Georgetown thrust footwall, east of the Georgetown–Middle Fork fault, contains a nearly complete Belt Supergroup section, with Piegan Group strata (Ypnm) overlain by a succession typical of the Missoula Group (Ymim). In the Georgetown thrust hanging wall, west of the Georgetown–Middle Fork fault, the Piegan Group grades up to sandy Lemhi strata instead.

The Johnson thrust and Maurice Mountain thrust are exposed along the eastern edge of the map and within the Foolhen Complex. Their traces have also been obscured by Tertiary normal faults (e.g., Fourth of July fault), but their hanging walls and footwalls also contain different stratigraphic sections. The Maurice Mountain footwall contains only a very thin (500 m, 1,600 ft) Belt section consisting of the Black Lion Formation. The hanging wall is the Grasshopper thrust plate (Ruppel and Lopez, 1984), which contains a very thick (>5,000 m, 16,000 ft) section of Lemhi Subbasin strata that was deposited within the Belt Basin.

Folds and Fabrics in the Footwall of the ADZ

The footwall of the ADZ in the north-central and northeastern parts of the quadrangle consists of metamorphosed, intensely deformed but still recognizable, Belt Supergroup strata that have several foliations and fold generations and are extensively intruded by Cretaceous to Tertiary plutons. The Anaconda Range in the Wisdom and Philipsburg (Lonn and others, 2003) quadrangles exposes the entire Belt Supergroup and lower Paleozoic sections in a large, broad, generally north–northwest-dipping homocline that has several foliations and superposed fold generations.

A layer-subparallel transposition foliation, S_1, is the most prominent foliation in the Anaconda Range (Desmarais, 1983; Lonn and others, 2003; Lonn and McDonald, 2004a; Neal and others, 2023a). It appears to be associated with and responsible for the tectonically thinned stratigraphic section observed in the Anaconda Range (Lonn and others, 2003). The stratal thinning was accomplished by nearly bedding-parallel zones of both coaxial and non-coaxial shear that display no obvious stratigraphic discontinuities and by distinct, bedding-parallel faults that omit stratigraphic sections. The folded Sawed Cabin detachment fault in the north-central part of the map is one such fault. It places the younger Missoula Group over the older Piegan Group (see fig. 4), omitting the lower part of the Missoula Group section. Broader zones of ductile shear without obvious stratal omission can be seen throughout the stratigraphic section, where high-strain zones alternate with unstrained or less-strained zones. The high-strain zones can display nearly bedding- or

Figure 4. The Sawed Cabin detachment fault juxtaposes brown Piegan Group on the left against light-colored quartzite of the upper Missoula Group on the right, omitting lower Missoula Group strata. Note sheared Piegan Group rocks left of the camera case grade to bedded Piegan Group strata in the upper left. Location N. 45.9347°, W. -113.5110°.

layer-parallel mylonitic foliation, boudinaged beds, flattened and stretched grains, rootless isoclines, and sheath folds (figs. 5A–5E). Lonn and McDonald (2004a) observed that Belt unit thicknesses varied greatly over short distances, suggesting boudinage on a kilometer scale.

The tectonic origins of S_1 and the stratal thinning have been difficult to explain. Lidke and Wallace (1992) and Wallace and others (1992) mapped a system of younger-over-older thrusts to explain the omitted and thinned section, whereas Lonn and others (2003) and Lonn and Johnson (2010) thought that Cretaceous synorogenic extension or lateral plastic flow were better explanations. Rare kinematic indicators in S_1 that show a generally top-to-the-west shear sense (Lonn and Johnson, 2010) and west-verging folds are common in the Anaconda and Flint Creek Ranges. Possible mechanisms for large-scale, hinterland-verging structures in the Anaconda and Flint Creek Ranges include non-coaxial shear between a ductile middle crust and rigid upper crust (e.g., Culshaw and others, 2006), and sinistral transpression along the Lewis and Clark Line driven by terrane accretion to the far west (Neal and others, 2023b).

Fishtrap Nappe (F_1 and S_1?)

The Fishtrap Fold Nappe, first described by Flood (1974), is a tens of kilometers-scale recumbent anticline exposed in the north-central part of the map. It closes to the northwest, and where it is best exposed, the axial plane has been tilted westward by subsequent fold generations (figs. 6A–6D), exposing its lower, overturned limb over a large area and creating complicated map patterns. The S_1 transposition foliation appears to be parallel to its axial plane, and appears to cut across its hinge, leading Neal and others (2023b) to propose that they developed coevally. It is unknown whether the Fishtrap fold is a local feature or a crustal-scale feature that underlies the entire northeastern part of the Anaconda Range, with the lower Belt strata exposed in the core of the fold. West-verging folds north of the quadrangle in the Flint Creek Range (Gwinn, 1960, 1961; Mutch, 1960, 1961; Lonn and others, 2003) might be related to the Fishtrap Nappe.

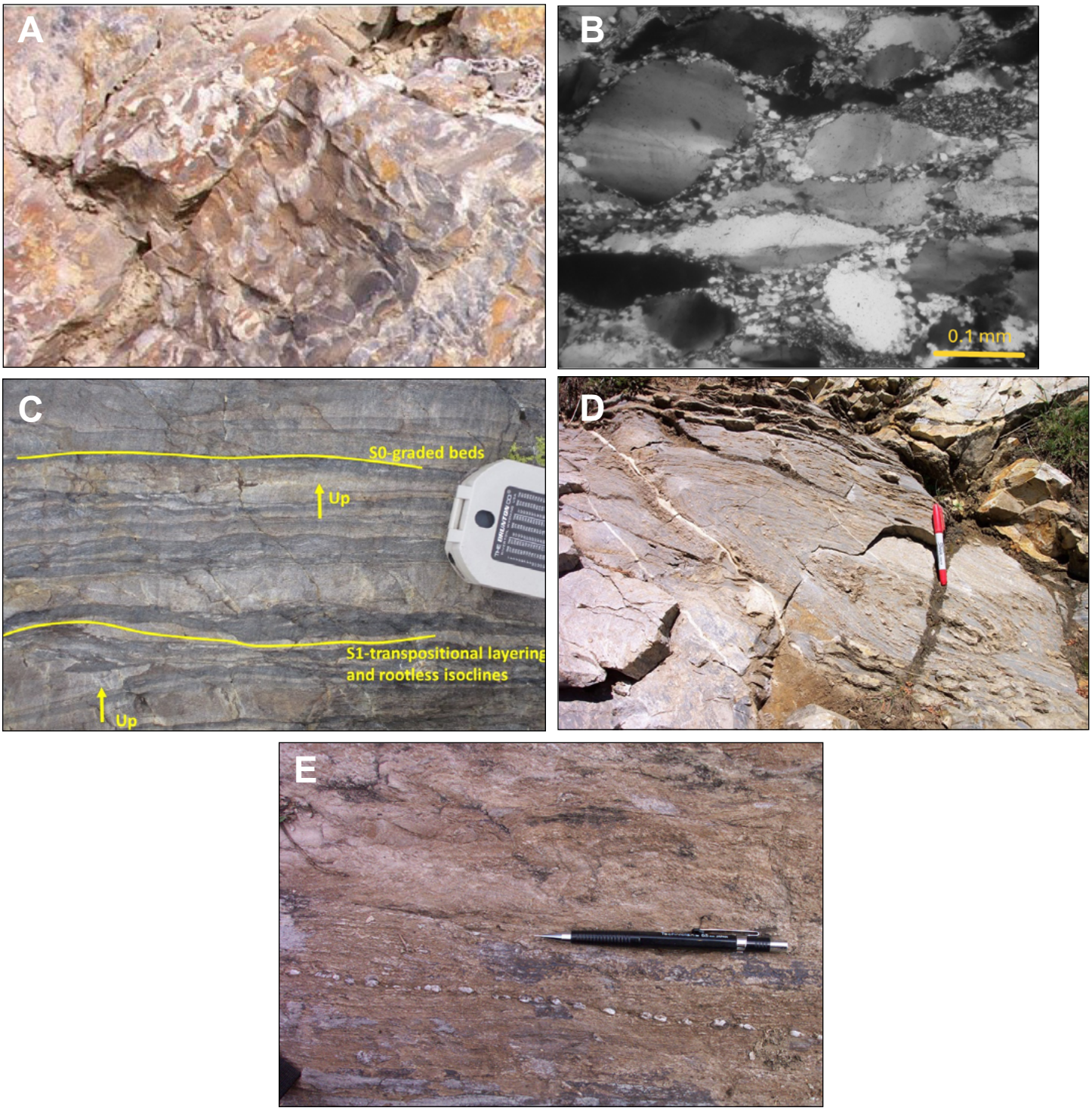

Figure 5. F_1/S_1 structures and stratal thinning in the Anaconda Range. (A) Mylonitic S_1 transposition foliation alternates with intervals where original sedimentary features are preserved. In the footwall of the ADZ, the transposition foliation accomplished significant stratal thinning throughout the sedimentary section. Later deformation formed cross-cutting S_2 foliation and F_2 folds at all scales. Red Lion Formation (unit Ꞓrlh), north-adjacent Philipsburg 30' x 60' quadrangle. Location N. 46.1686º, W. -113.2214º. (B) Photomicrograph of flattened quartz grains in Missoula Group quartzite (unit Ymim) that were deformed during tectonic thinning and development of the S_1 transposition foliation. Note that the quartz porphyroclasts are elongate, exhibit undulose extinction, have serrated edges, and are mantled by microcrystalline grains. Sample collected at N. 45.9874º, W. -113.5167º. (C) Graded beds (S_0) above and below transposed and isoclinally folded layer show same stratigraphic facing. Rootless isoclines are common and typically confined to thin layers or individual beds. Upper Prichard Formation (unit Ypm) near Lost Lakes, location N. 45.9603º , W. -113.3724º. (D) Sheath fold resulting from layer-parallel shear developed within a limestone bed in the Piegan Group (unit Ypnm). No primary structures are preserved within the sheath fold, but strata above and below it preserve original sedimentary structures that show the same way up. Location N46.0566º, W-113.2763º. (E) Thin quartz vein dismembered by S_1 layer-parallel shear that resulted in stratal thinning. Piegan Group (unit Ypnm). Location N. 45.9295º, W. -113.5162º.

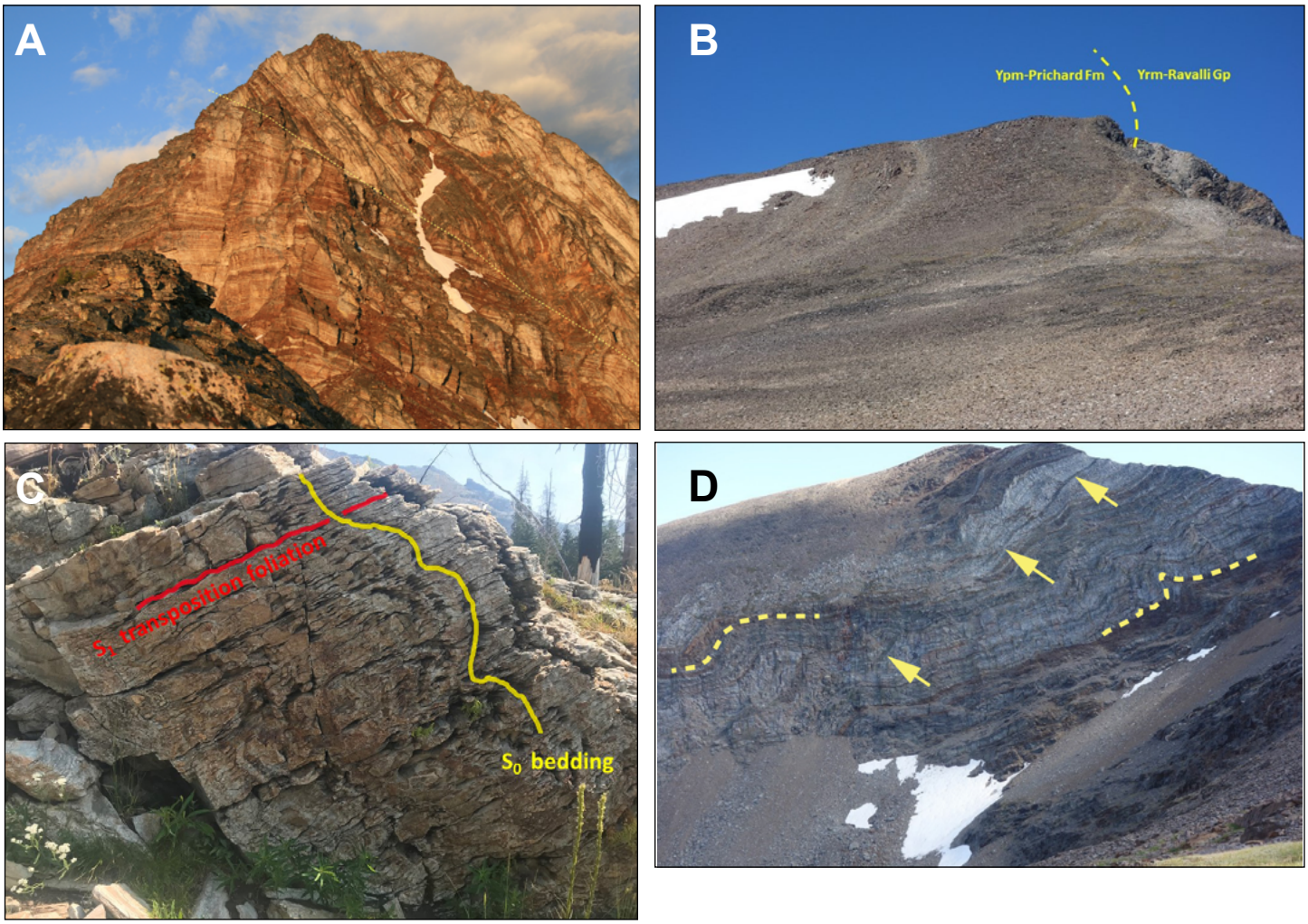

Figure 6. Fishtrap Nappe. (A) Southward view of the Fishtrap recumbent anticline on the near-vertical north face of the unnamed peak immediately west of Warren Peak. The axial surface (dashed line) is tilted downward towards photo right (west) in the limb of a north-trending, upright F_2 fold (Lonn and others, 2003; Neal and others, 2023a,b). Location N. 45.9813º, W. -113.4416º. (B) Westward view of the Fishtrap recumbent anticline hinge area on West Goat Peak. Stratigraphic facing is to the right. Light-colored rocks of the Ravalli Group (unit Yrm) are quartzite beds; light-colored rocks within the Prichard Formation (unit Ypm) are calc-silicate beds. Location N. 45.9622º, W. -113.3940º. (C) Outcrop within the hinge zone of the Fishtrap anticline with steeply dipping bedding (yellow line) and cross-cutting S_1 foliation (red line). S_1 does not appear to be folded around the hinge, and instead is nearly parallel to the fold's axial plane, suggesting that the fold and S_1 formed coevally. Southward view on the south face of the unnamed peak east of Warren Peak. Location N. 45.9797 º, W. -113.4517º. (D) Southward view of the north face of East Goat Peak (N. 45.95753, W. -113.38002), illustrating the structural complexity in the Anaconda Range. Here, Prichard Formation beds (unit Ypm) are overturned in the lower limb of the Fishtrap fold and dip 30° away from the camera. Beds have been subsequently deformed by small-scale north–south-trending F_2 folds (dashed lines) that here appear to be east-verging, but in many other areas verge west. Also note dark-colored cross-cutting dikes with apparent east dips (arrows).

Second Generation Folds and Fabrics (F_2 and S_2)

At least one later generation of generally north-trending folds and related axial-plane cleavage postdates the transposition foliation S_1 and the Fishtrap Nappe. These folds dominate the map patterns along the north-central border of the quadrangle and on the north-adjacent Philipsburg quadrangle (Lonn and others, 2003). Many of the folds are asymmetric and verge west, although a few verge east. Axial plane cleavage S_2 is often conspicuous (fig. 7), and dominantly dips to the east. The transposition foliation, S_1, is folded around the hinges of these folds, and both the Georgetown thrust and the Fishtrap Nappe are folded by F_2.

Neal and others (2023a,b) describe F_2 in the Anaconda Range as upright folds produced by the same progressive deformation as F_1. Desmarais (1983) describe F_2 and S_2 in the Chief Joseph Complex as transposing F_1 and S_1 into northwest-striking isoclines with a steeply south southeast-plunging lineation.

Figure 7. Small-scale F_2 folds in Piegan Group strata (unit Ypnm), with strong S_2 axial planar cleavage (solid line). Note that cleavage is crenulated by poorly understood F_3 folds. Location N. 45.9387°, W. -113.5445°.

These two interpretations are compatible, and Desmarais' analysis emphasizes that the initial orientation of F_1/S_1 structures cannot be determined since they are now transposed into a F_2/S_2 orientation.

Minimum ages of the complex F_1 and F_2 structures are constrained by the ages of cross-cutting Late Cretaceous plutons (Desmarais, 1983; Wallace and others, 1992; Lidke and Wallace, 1992). The 72 Ma (this study) Martin Creek Pluton has foliation developed near its margins that is parallel to foliations in the country rock and is thus probably syntectonic (Lonn and McDonald, 2004a). The Storm Lake Pluton immediately north of the Wisdom quadrangle that cross-cuts S_1 in some places and appears to be deformed parallel to it in others is older, with an age of approximately 75 Ma (Grice, 2006).

Grice (2006) concluded that the peak high temperature–low pressure metamorphism of the Anaconda Range occurred ca. 75 Ma, consistent with other studies (Flood, 1974; Wiswall, 1976; Haney, 2008).

F_3 and S_3

Desmarais (1983, p. 43) described a northwest-trending foliation in Tgbm of the Chief Joseph Complex, as a penetrative "joint/fracture system." We interpret the foliation as S_3, a disjunctive (spaced) cleavage with discrete domains (in the sense of Borradaile and others, 2012); that is, penetrative on a hand-sample scale (i.e., is pervasive, with a spacing of less than 1 cm; fig. 8). S_3 is strongest in the 63 Ma (this study) Trail Creek Pluton, though it occurs locally in all Tgbm bodies.

The close spacing of the cleavage domains suggests formation in response to compressive rather than extensional stresses and that Tgbm was intruded in the latest stage of regional shortening. This might indicate that the intrusion of Tgbm was not associated with crustal collapse and extension, as is implied by other workers (e.g., Foster and others, 2010; Howlett and others, 2021).

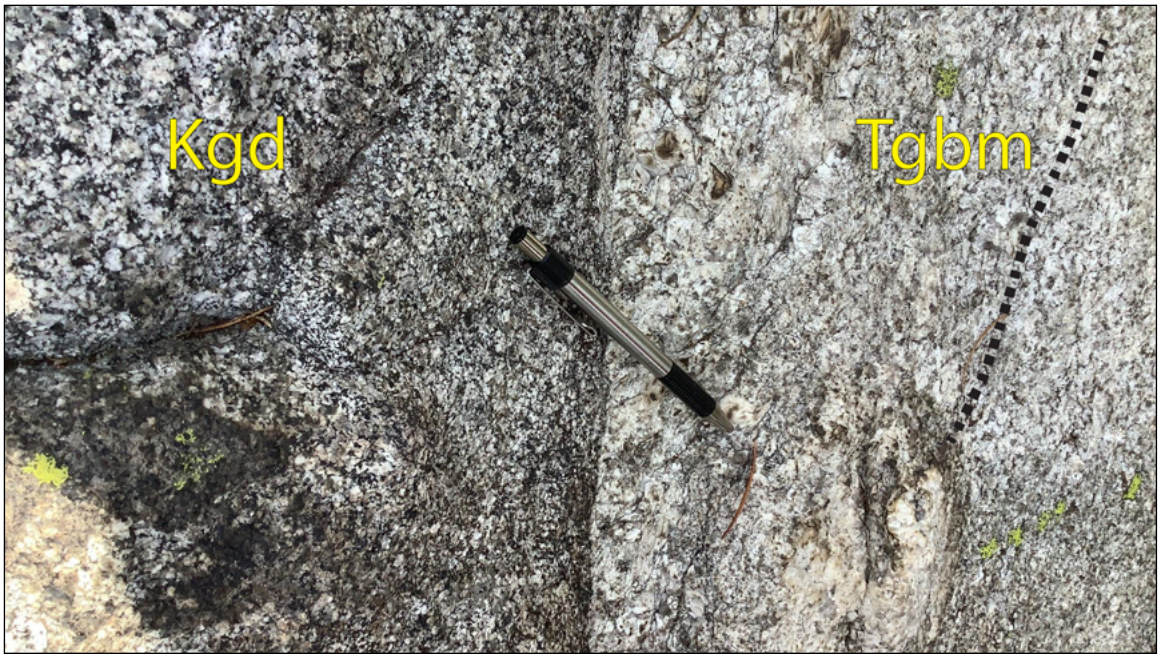

Figure 8. Cretaceous granodiorite (unit Kgd) in sharp contact with Tertiary two-mica granite on the right (unit Tgbm) in the Chief Joseph Complex. Tgbm is deformed adjacent to the contact and an S3 disjunctive cleavage is traced by the dashed line.

Folds and Fabrics in the Foolhen Complex

F_1 and F_2 in the Foolhen Complex in the West Pioneer mountains are similar to the Chief Joseph Complex and Anaconda Range, i.e., S_1/S_2 transposition fabrics and layer-parallel faults characterized by increased foliation intensity next to planes across which strata are either eliminated or repeated. In the Foolhen Complex, the transposition foliation also parallels contacts like those between the gneiss of Foolhen Ridge (Kgn), Kqsg, and Kgdf, which do not appear to be faults and where the lack of asymmetric structures suggests a pure shear strain history. Small rootless isoclines are common, and overprinting structures demonstrate more than two generations of transposition (figs. 9A, 9B).

Transposition is strongest in the noses of WNW-trending F_2 folds like the one responsible for the canoe-shaped trace of the Johnson thrust in the center of the map's northeast quadrant. F_1/F_2 progressive deformation is associated with migmatization and intrusion of Kgdf, which in the Foolhen Complex is dated ca. 73 Ma by zircons in Kgdf and Kgn (table 1).

Open, upright, northeast-trending F_3 folds refold the large antiform and synform in the Foolhen Complex. Local S_3 crenulations and mesoscopic F_3 folds commonly plunge northeast. F_3 in the Foolhen Complex is perpendicular to F_3 in the CJS, and it is unclear how the two might be related.

Tertiary Anaconda Detachment Zone (ADZ)

O'Neill and others (2004) discovered that a low-angle detachment fault, the ADZ, bounds the east and southeast sides of the Flint Creek and Anaconda Ranges. O'Neill and others (2004) identified the footwall as the Anaconda Metamorphic Core Complex (AMCC). This report brings some aspects of the AMCC model into question, however, suggesting the ADZ footwall does not fit a traditional metamorphic core complex (MCC) model. First, metamorphism in the "core" of the AMCC is Cretaceous (Grice, 2006; Haney, 2008) and predates the proposed 53 Ma initiation of extension (Foster and others, 2010) by around 20 Myr. Second, rather than separating a metamorphic core from an unmetamorphosed hanging wall, the ADZ transects the metamorphic complexes, separating the Chief Joseph Complex from rocks of the same grade in the Foolhen Complex. Further, peraluminous two-mica granites that have been associated with the AMCC "core" have now been found in the ADZ hanging wall in the West Pioneer Mountains (62.8 ± 1.0 Ma Tgbm, CE19PH11a, table 1).

Extension in the region appears to have begun with top-to-north–northeast extension, represented in the north end of the Big Hole basin by roughly east–west-trending, north-dipping normal faults that expose Precambrian rocks in their footwall. Early top-to-north–northeast strands of the ADZ are also found

Figure 9. Multi-generation transposition in the Foolhen Complex. (A) Foliated Cretaceous granodiorite orthogneiss (unit Kgdf) with transposed gneissosity. A block with older gneissic layering (S_1) is sharply bounded by a perpendicular, more diffuse, transposition foliation (S_2). (B) Intermediate phase of transposition in migmatite (unit Yqsg). Folded partial melt leucosomes in Yqsg (roughly parallel to vertical sides of photo) are overprinted by new leucosomes parallel to the pencil that are axial planar to folds in first-generation leucosomes.

at the north end of the Flint Creek Range, around Mount Powell, and on the north flank of Mount Hagan (Scarberry and others, 2019; Elliott, 2019). The old east–west extensional faults are cut by the northeast-trending detachment faults that define the southeastern front of the Anaconda Range. O'Neill and others (2004) and Foster and others (2010) report that extension on the ADZ was towards the east–southeast, but Howlett and others (2020) measured extension lineations near Pintler Lake (north central part of the map) that vary in trend from east to south–southwest, with a mean plunge and trend of 19º towards 138º. In the Big Hole Battlefield area, at the southernmost extent of the ADZ, Elliott (2024) found an even wider distribution of extension directions on mostly gently east-dipping fault planes.

In the Big Hole Valley, extension on the ADZ continued into the Miocene and cut the Sixmile Creek Formation (Tsc). This counters previous studies that place the end of low-angle extension before Miocene high-angle Basin-and-Range-style extension (e.g., Janecke, 2007; Sears and others, 2009; Foster and others, 2010). In the Wisdom quadrangle the younger, steeper normal faults in the Big Hole Valley are mutually cross-cutting and there is not obvious temporal transition from low-angle to high-angle faulting.

Continued extension across the region on numerous high-angle normal faults has deepened basins like the Big Hole Basin, the Wise River Valley in the southeastern part of the map, and the French Basin in the northwestern part of the map.

MINERALIZATION

There are no active mines within the Wisdom 30' x 60' quadrangle. Abandoned mines are small and few, though there are many prospects. Most are within contact zones of intrusive rocks, or are placer deposits within Quaternary or Tertiary alluvial deposits.

West Pioneer Range

Berger and others (1983a,b) assessed the central West Pioneers for mineral potential and concluded there is moderate to high potential for molybdenum, gold, and silver, low to moderate potential for copper, zinc, and lead, and low potential for tungsten and placer gold.

At the north end of the West Pioneers are scheelite-bearing skarns of the Calvert Hill District, where Cretaceous and Tertiary granitoids intruded Paleozoic carbonates (Messenger, 2016; Messenger and Gammons, 2017). The Calvert Mine (also known as "Red Buttons") was a significant producer of tungsten. Between 1956 and 1962, approximately 113,000 tons of ore grading 1.1% WO_3 were mined from an open pit (Walker, 1963; Geach, 1972). Additional unmined reserves exist at depth. The site is now a popular destination for mineral collectors seeking epidote, garnet, beryl, and scheelite from the mine dumps (Gobla, 2012).

Worthington (2007) reported on molybdenum deposits and prospects in the south part of the West Pioneer Range. These include the Stonehorse prospect near Lacy Creek, the Armor Creek prospect between Odell Creek and Anderson Meadows, and the Tim Creek prospect on the Big Hole–Wise River divide and headwaters of Stewart Creek. The prospects cover large areas of Belt Supergroup and intrusive rocks and are weakly anomalous in molybdenum and copper. None have been developed as economic deposits.

In the westernmost West Pioneers, in the Wisdom District of Loen and Pearson (1989), are small gold- and silver–bearing quartz-pyrite veins that cut plutonic rocks. Production from these veins has been small. Nearby, defunct placer workings are scattered along Steel Creek and its tributaries (Geach, 1972).

Northern Beaverhead Range

The southwest quarter of the Wisdom quadrangle contains the Pioneer, or Rescue district, the Lost Trail district, and the Gibbonsville district of Loen and Pearson (1989).

Anomalous silver, copper, and iron concentrations are found in the Moosehorn Mine and Jumper No 1 prospects south of Wenger Creek, which is a small tributary to Ruby Creek (Geach, 1972). The deposits are characterized by massive specular hematite and quartz veins in the Swauger Formation Ysw.

In the headwaters of the North Fork of the Salmon River in Idaho, anomalous gold and copper are hosted by Mesoproterozoic quartzite and argillite. The ore is in narrow, east-trending veins broken by faults. The primary vein minerals are auriferous pyrite and chalcopyrite in a gangue of quartz and local calcite. Stewart and others (2025) describe the Koper Kyute copper prospect in Belt-aged quartzite and calcsilicate (Yqcs) between Pierce Creek and the Continental Divide.

East of the continental divide, Placer Creek, Trail Creek, Cow Creek, May Creek, and Ruby Creek have been worked for placer deposits in remnants of Tertiary gravel and Quaternary alluvium. Production has been small (Loen and Pearson, 1989). Placer deposits west of the divide near Gibbonsville were more productive (Loen and Pearson, 1989).

Elliott (2024) described a barite showing in volcanogenic sediments (Tvs) near Johnson Creek (Sample site CE20BHB8).

Bitterroot River Headwaters

Only a few mineral occurrences are known in the Sula area in the northwest corner of the map. Loen and Pearson (1989) report beryl occurrences, about which little is known and locations are vague.

Anaconda Range

In the Moose Lake district of Loen and Pearson (1989) on the north edge of the Wisdom quadrangle, Mesoproterozoic sedimentary rocks intruded by Cretaceous and Tertiary granitoids host mineralized quartz veins. The Senate Mine produced small amounts of copper and lead (Loen and Pearson, 1989). Loen and Pearson (1989) also report molybdenum, silver, and tungsten showings near Lower Seymour Lake on the northeast edge of the map area. Alluvium in the headwaters of French Gulch and its tributaries in the northeast corner of the map area host placer gold deposits that were extensively developed in the 19th and early 20th centuries.

DESCRIPTION OF MAP UNITS

Quaternary and Tertiary Sediments and Rocks

Qal **Alluvium (Quaternary: Holocene)**—Gravel, sand, silt, and clay in channels of modern rivers and streams. Clasts generally subrounded to well-rounded, resistant rock. Composition varies depending on source of clasts. Variable thickness, typically less than 10 m (30 ft).

Qaf **Alluvial fan deposit (Quaternary: Holocene and Pleistocene?)**—Gravel, sand, silt, clay, with local ash beds; poorly sorted with large clasts, matrix-supported or clast-supported. Debris flow components may contain angular clasts, and distributary components may contain rounded clasts. Deposits have retained significant evidence of original alluvial fan morphology. Mapped Qaf deposits are not necessarily age-equivalent. Variable thickness, typically less than 15 m (50 ft).

Qls **Landslide deposit (Quaternary: Holocene–Pleistocene)**—Mass-wasting deposits consisting of unsorted mixtures of clay to boulder-size clasts. Includes rotated or slumped blocks of bedrock and surficial sediment, earthflow deposits, and mudflow deposits. Color and lithology reflect that of parent rocks and transported surficial material. Deposit may be stable or unstable, and mapped landslides are not necessarily age equivalent. Variable thickness, typically less than 60 m (200 ft).

Ql **Lake deposit (Quaternary: Holocene–Pleistocene)**—Clay, silt, and sand in very thin beds and varves, deposited behind moraines and in glacially scoured depressions. May include swamp deposits. Thickness is probably less than 15 m (50 ft).

Qpa **Paludal deposit (Quaternary: Holocene–Pleistocene)**—Organic plant matter accumulated in swamp, marsh, or wet meadow. Thickness is less than approximately 10 m (33 ft).

Qta **Talus (Quaternary: Holocene–Pleistocene)**—Coarse, unconsolidated, angular, locally derived clasts in apron-like deposits below steep slopes. May include rock-slide deposits. Variable thickness, generally less than 10 m (33 ft).

Qalo **Alluvium, older than Qal (Quaternary: Holocene? and Pleistocene)—**Gravel, sand, silt, and clay in older channels of rivers and streams. Clasts generally subrounded to well-rounded, resistant rock. Composition varies depending on source of clasts. Surfaces of Qalo deposits are 1 to 10 m (3 to 30 ft) above the modern floodplain. Variable thickness, typically less than 10 m (30 ft).

Qg **Glacial deposits, undivided (Quaternary: Pleistocene)**—Primarily poorly sorted, unconsolidated till and subordinate outwash; also locally includes other types of glacial deposits. May be hummocky, bouldery deposits with clasts as large as 3 m (10 ft) in diameter. Variable thickness, typically less than 45 m (150 ft).

Qgt **Glacial till (Quaternary: Pleistocene)**—Unsorted clay to boulder deposits in lateral, ground, and medial moraines. Characterized by hummocky terrain scattered with large subangular to subrounded boulders up to 3 m (10 ft) in diameter. Variable thickness, typically less than 60 m (200 ft).

Qgto **Glacial till older than Qgt (Quaternary: Pleistocene)**—Unsorted clay to boulder deposits in lateral, ground, and medial moraines. Characterized by hummocky terrain that is

more subdued than Qgt, and contains more heavily weathered boulders. Variable thickness, typically less than 60 m (200 ft).

Qgo **Glacial outwash (Quaternary: Pleistocene)**—Stratified to weakly stratified sand and gravel interpreted to be deposited in drainages below end moraines during deglaciation. Clasts may be as large as boulder size. Variable thickness, typically less than 30 m (100 ft).

Qgoo **Glacial outwash, older than Qgo (Quaternary: Pleistocene)**—Stratified to weakly stratified sand and gravel, interpreted to be deposited during deglaciation in drainage below end moraine. Younger outwash channels incise surfaces of Qgoo deposits. Variable thickness, typically less than 30 m (100 ft).

QTaf **Alluvial fan deposits (Quaternary: Pleistocene, or Tertiary: Pliocene?)—**Poorly to well-sorted, rounded to subangular boulders, cobbles, sand, silt, and clay. Clasts derived from adjacent uplands. Surfaces of QTaf deposits have a distinct fan shape and now stand more than 15 m (50 ft) above modern deposits. Thickness as much as 30 m (100 ft).

QTls **Landslide deposit (Quaternary or Tertiary)**—Mass-wasting deposit of unsorted clay to cobble-size sediment. Color and lithology reflect the parent rocks and transported surficial material. One deposit near Big Hole Battlefield.

QTgr **Gravel (Quaternary or Tertiary)**—Isolated fluvial gravel deposits in patches that cannot be stratigraphically connected to other sedimentary deposits. Clasts dominated by well-rounded quartzite and other resistant lithologies.

Ts **Sediments, undivided (Tertiary)**—Poorly exposed, generally fine-grained, tan to white sediments with scattered pebbles and cobbles and lacking stratigraphic context. Includes minor fluvial gravels with rounded cobbles and pebbles. Forms low hills in flat-lying farmland near the west edge of the map.

Tgr **Gravel (Tertiary)**—Poorly exposed cobble and boulder gravel in sand and silt matrix, lacking stratigraphic context, mostly expressed as lag deposits. Clasts are angular to well-rounded, and may have tan-weathering rinds. Clasts are mostly metamorphic rock types and granite, dominated by quartzite. Characterized by smooth, rounded topographic surfaces. Tgr along the Big Hole River and Deep Creek has close-spaced, well-rounded clasts and appear to be fluvial deposits. Thickness less than 65 m (220 ft).

Tdf **Debris-flow deposits (Tertiary)**—Boulder and cobble gravel with unsorted, angular to well-rounded clasts up to 2 m (6 ft) across. Angular clasts are dominated by local rock types, and rounded clasts are dominated by quartzite, indicating they had a long transport history. Exposed in Goris Gulch and Christianson Creek near the center of the map. Thickness varies from less than 10 m (30 ft) to as much as 300 m (1,000 ft).

Tsc **Sixmile Creek Formation and equivalents (Tertiary: Miocene)**—Boulder and cobble gravel with prominent rounded to well-rounded quartzite clasts. Clasts are poorly to moderately sorted, and up to 40 cm (16 in) across. Mostly occur as lag deposits but cobbles are locally imbricated, suggesting that they are in outcrop. Miocene age indicated by stratigraphic position above Paleogene units (Tre and Tba), tentative fossil identifications (Roe, 2010), and detrital zircon spectra that give MDAs of 11.6 Ma (Roe, 2010), 51.5 ± 0.6 and 10.8 ± 0.4 Ma (CE20BHB18, CE23W100K10, table 1). Thickness up to 120 m (400 ft).

Tba **Basalt (Tertiary: Oligocene)—**Dark gray vesicular to non-vesicular glassy basalt to basanite flows with olivine and plagioclase phenocrysts and brown to gray welded tuff. Xenoliths and zircon xenocrysts are common. Two prominent basalt flows are interlayered with upper Tre in the northern part of the Pine Hill 7.5' quadrangle. Fritz and others (2007) report a K-Ar age of 21.9 ± 0.3 Ma for one of these flows. U-Pb zircon separates for three samples of Tba (23RDS09, 23RDS10, and 23RDS11, table 1) have inherited zircons ranging between ca. 1,700 Ma and 25 Ma. Sample 23RDS10 gives an MDA of 52.4 ± 0.3 Ma, but the weighted mean of the 11 youngest concordant grains from the three combined samples

is 25.6 ± 0.3 Ma, which we consider the most reasonable age for this unit. The age and composition of Tba suggest it is part of the upper Dillon Volcanic Suite (Fritz and others, 2007).

Tre **Renova Formation and equivalents, undivided (Tertiary: Eocene through Oligocene)**—Poorly exposed white, gray, and orange ashy clay and silt, with local sand and gravel lenses. Some fine layers contain matrix-supported sand grains and sparse cobbles. Coarse clasts may be matrix- or clast-supported. Locally olive green, brown, and gold when wet. It contains gray paleosols near the top, some wood fragments, and ochre to maroon iron stains. Clay intervals weather with a characteristic popcorn texture. In the Wisdom 30' x 60' quadrangle, Tre has yielded U-Pb zircon MDAs of 26.2 ± 0.4, 26.4 ± 0.1, 31.7 ± 0.8 Ma, and 51.9 ± 0.6 (CE22BHB01, CE21WE02, CE19PH5, CE20BHB17, table 1). A tooth fragment found at Chalk Bluff was tentatively dated as Oligocene (Hanneman and Nichols, 1981; Roe, 2010). Roe (2010) reports U-Pb zircon TIMS ages of 29.60 ± 0.008 Ma, for ash in the northwest corner of the map. Thickness up to 120 m (400 ft).

Trcp **Cabbage Patch Member of the Renova Formation (Tertiary: Oligocene)**—Pale-colored, poorly to non-lithified clays, silts, tuffs, with well-lithified channelized sandstone and conglomerate. Detrital and life-position carbonized wood scattered throughout. Clays are commonly tuffaceous with pervasive yellow and orange mottling and blocky fracture. Silicified mudstone, sandstone, and conglomerate are brown to orange, coarse, lithic, feldspathic, and contain single large euhedral flakes of biotite and muscovite. Sandstone and conglomerate form trough crossbedded lenses from less than a meter (3 ft) to more than 4 meters (13 ft) thick. Pebbles and cobbles commonly imbricated. The coarse clastic lenses are most abundant at the top of the exposed unit and form steep banks along Deep Creek in the northeastern part of the map area. Crossbedded lenses of well-lithified lithic sandstone and conglomerate with euhedral feldspar, biotite, and muscovite grains are a distinctive feature of the Cabbage Patch Member more than 100 km (60 mi) north of the Wisdom 30' x 60' quadrangle (Calede and Rasmussen, 2015) to at least 140 km (85 mi) south (Elliott and Lonn, 2016). Thickness is unknown, but is probably less than 90 m (300 ft).

Tj **Jasperoid breccia (Tertiary)**—Large blocks of Cambrian quartzite and carbonate with red and brown cryptocrystalline quartz cement and veins. One exposure in the northeastern corner of the map.

Tvs **Volcanic sediment (Tertiary: Eocene)**—Sedimentary facies of the Lowland Creek and Challis volcanic suites. In the northeastern corner of the quadrangle Tvs is mostly expressed as gravel lag in tuffaceous soils and green-cemented lahar deposits. Clasts include red and caramel-colored chert, course crystalline marble, hornblende aplite, red, pink, and green quartzite, fine-grained limestone, hornblende granodiorite, and rhyolite and dacite from map units Tlc and Tcv.

In the western part of the quadrangle, Tvs is poorly exposed and mainly occurs as float in brown and gray clay-rich soils. Includes conglomerate, sandstone, and claystone, with thin rhyolite and rhyolite ash layers. Color varies from light gray to light reddish gray, locally red, weathering to pale yellow. Loose, rounded cobbles are commonly broken. Forms rare large shelves or boulders of silica-cemented, clast-supported, pebble–cobble conglomerate. Clasts include biotite–muscovite granite (unit Tgbm), chalcedony, frosted quartz, feldspar, mica crystals, rhyolite (white to pink including quartz-eye tuff and red porphyry), rounded feldspathic quartzite (Belt Supergroup), mica schist, and aplite.

A U-Pb zircon MDA of 64.5 ± 1.2 was obtained from interbedded feldspathic siltstone and sandstone near Johnson Creek west of the center of the Wisdom quadrangle (CE20BHB8, table 1), and a rare layer of light gray to white, variably welded, quartz–biotite–muscovite–feldspar crystal tuff interlayered with Tvs at Battle Mountain (CE20BHB02, table 1) yielded a U-Pb zircon age of 51.4 ± 1 Ma. Tvs is the oldest Cenozoic sedimentary unit reported

in southwest Montana. Thickness is over 600 m (2,000 ft) at Battle Mountain.

Tcv **Challis Volcanic Group (Tertiary: Eocene)**—Rhyolite and dacite tuff, flows, and dikes interbedded with unconsolidated tuffaceous fluvial sands and cobble gravel. Rhyolite tuff is tan, poorly welded to flow-banded and pumiceous, with phenocrysts of quartz, plagioclase, and sanidine (Lopez, 1982). Dacite is red-brown to gray biotite–hornblende tuff. Phenocrysts of plagioclase, biotite, and hornblende constitute 5 to 15 percent of the rock. Prominent layering is interpreted as compaction during welding, though the dacite may be flows rather than tuff. A rhyolite tuff in the southwestern corner of the map area has a U-Pb zircon age of 49.0 ± 0.2 Ma (23RB430, table 1).

Tbdt **Biotite dacite tuff (Tertiary: Eocene)**—Light gray to tan, moderately welded dacitic ash to lapilli tuff. Characterized by dark quartz crystals as large as 3 mm and sparse but ubiquitous crystals of biotite and hornblende smaller than 1 mm. Heterogeneous with varied proportions of crystals, lithics, and pumice. Crystals, which compose 10 to 30 percent of the rock, are predominantly white plagioclase as large as 5 mm. Subordinate quartz is commonly dark and as large as 3 mm. Pseudohexagonal biotite and acicular hornblende, as much as 3 percent, are small (<1 mm). Rounded volcanic lithics as large as 6 cm, similar to matrix but lighter in color, compose 0–40 percent of the rock. Rounded pumice as large as 1 cm is rare but locally composes up to 20 percent of the rock. The tuff rests on an eroded surface of the East Fork Dike Swarm (unit Tdsr) and is cut by both rhyolite and dacite dikes. Tbdt has a U-Pb zircon age of 52.2 ± 0.4 Ma (AH21WW4, table 1).

Tlc **Lowland Creek volcanic rocks, undivided (Tertiary: Eocene)**—Unconsolidated light gray to white tuffs intermixed with gray, pink, red, and green aphanitic dacite and rhyolite and fine to coarse clastic sediments (Tvs). Typically has abundant quartz eyes and euhedral phenocrysts of potassium feldspar, biotite, and some hornblende. Locally flow banded or scoriaceous. Only mapped in the northeastern corner of the Wisdom quadrangle where it is contiguous with the mapped extent of the Lowland Creek Volcanic field (Scarberry and others, 2019). Tlc is otherwise indistinguishable from Tcv. Dated at 53–48 Ma (Dudás and others, 2010; Scarberry and others, 2019). Thickness is unknown in the Wisdom quadrangle, but is over 600 m (approximately 2,000 ft) in the northeast-adjacent Butte North quadrangle (Scarberry and others, 2019).

Tlcb **Lowland Creek volcanic breccia (Tertiary: Eocene)**—Distinctive gray dacitic autoclastic flow breccia in Tlc.

TKYhcs **Hell Roaring Creek Subcomplex (Proterozoic, Cretaceous, and Tertiary: Eocene)**—Closely intermingled migmatite, Mesoproterozoic quartzite, gneiss and schist, Cretaceous foliated granodiorite, Cretaceous granite, aplite, Paleogene two-mica granite, and Eocene dacite and rhyolite (map units Yqsg, Kgdf, Kg, TKa, Tgbm, Td, and Tr). Part of the Chief Joseph Complex. There are rare outcrops of mylonite and cataclasite in the subcomplex near the ADZ. Desmarais (1983) mapped parts of the subcomplex as the gneissic middle member of the Mount Shields Formation, i.e., strongly foliated quartzofeldspathic gneiss and pelitic schist that is migmatitic in places.

Veins, dikes, and sills in the subcomplex are variably deformed. Dacite (Td) and rhyolite (Tr) bodies are mostly tabular and may be brittlely deformed. Aplite and granitic veins can be ptygmatically folded isoclines and/or transposed with metamorphic layering in metasedimentary units.

Cross-cutting relationships and U-Pb geochronology in the subcomplex near the confluence of Hell Roaring and Mussigbrod Creeks (fig. 10) reveal the following sequence of magmatism and metamorphism, listed from oldest to youngest;

1. Migmatitic meta-sedimentary rocks—biotite–muscovite schist and gneiss with quartz–feldspar leucosomes and ptygmatic veins. Lithologically similar to metamorphosed Belt Supergroup

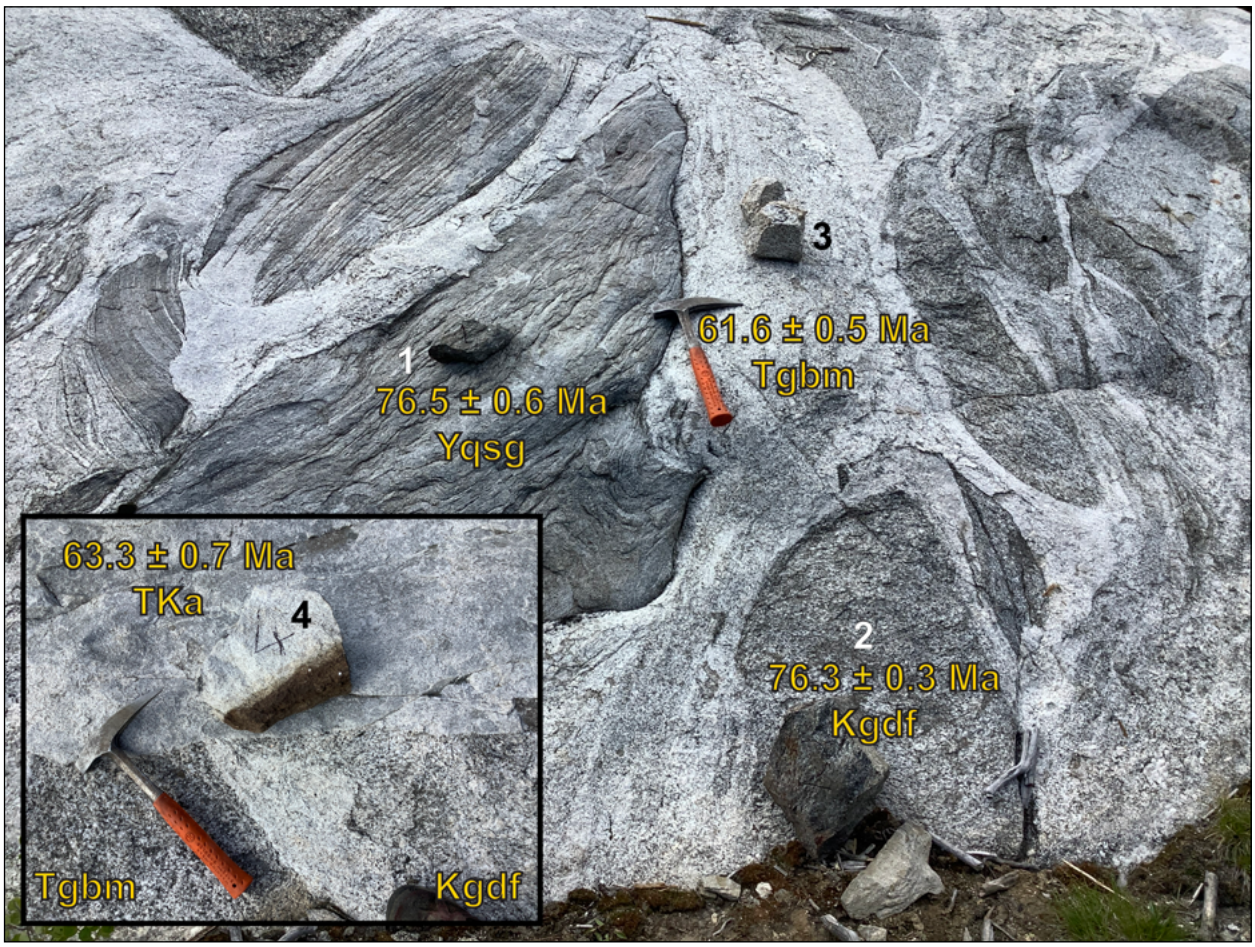

Figure 10. Dated phases in the Hell Roaring Creek Subcomplex (TKYhcs on map) with U-Pb zircon ages (samples CE20BP1-4, table 1). A dacite dike related to the East Fork Dike Swarm outside the frame of the photograph cross-cuts phases 1–4 and has a U-Pb zircon age of 51.7 ± 0.8 Ma (sample CE20BP5). Each of the dated samples is shown sitting on the phase from which it was collected, and numbered 1–4 from oldest to youngest based on cross-cutting relationships.

rocks (Yqsg) elsewhere in the map area; Cretaceous metamorphic age.

2. Biotite gneiss and granodiorite orthogneiss (Kgdf) with U-Pb zircon ages of 76.3 ± 0.3 and 76.5 ± 0.6 Ma (CE20BP1, CE20BP2, table 1). The orthogneiss is composed of 30–50 percent biotite and no hornblende. The gneissic foliation is defined by strong preferred orientation of biotite within millimeter- to centimer-thick compositional layering.

3. Coarse-grained, equigranular, biotite ± muscovite granite (Tgbm) with 5 to 10 percent biotite and muscovite. U-Pb zircon ages from this unit are 63.3 ± 0.6 Ma and 61.6 ± 0.5 Ma (CE18BP1, CE20BP3, table 1).

4. Aplite in fine-grained leucocratic dikes and veins (TKa), with a U-Pb zircon age of 63.3 ± 0.7 Ma (CE20BP4, table 1).

5. A dacite–rhyodacite dike (Td) that is tabular, sharp-edged, fine-grained, and porphyritic, with a U-Pb zircon ages of 51.7 ± 0.8 Ma (CE20BP5, table 1). The dike is related to the East Fork Dike Swarm.

A sheet of Kgdf within migmatitic metasedimentary rocks near Lost Trail Pass has a U-Pb zircon age of 76.8 ± 0.4 Ma (23RL030, table 1).

Tds **East Fork Dike Swarm (Tertiary: Eocene)**—Dikes and sills of tan, light pink, green, and gray dacite, rhyodacite, and rhyolite, commonly porphyritic with sanidine, plagioclase, quartz, biotite, and hornblende. Though chilled margins of dikes are commonly found, the host

rock is poorly exposed. The tabular bodies in the swarm generally strike northeast and dip steeply to gently to the northwest. Forms the East Fork Dike Swarm (Hyndman and others, 1977) with Tdsr.

One Tds dike yielded a U-Pb zircon age of 52.4 ± 0.4 Ma (AH21WW5, table 1; incorrectly identified as granodiorite, Mosolf and Kylander-Clark, 2023b). $^{40}Ar/^{39}Ar$ thermochronology of Tds bodies yielded cooling ages of 50–48 Ma (Badley, 1978; Desmarais, 1983; Simonsen, 1997; Bausch, 2013).

Tdsr **East Fork Dike Swarm, rhyolite dominant (Tertiary: Eocene)**—Aphanitic to porphyritic (Tr) dikes, with minor aphanitic to porphyritic dacite (Td) dikes and rare screens of country rock. Where exposed, dikes are tabular, less than 15 m (49 ft) thick, and are sub-vertical to northwest-dipping. Weathering to low, pinkish slopes that contrast sharply with the resistant dikes of Tds. Underlies biotite dacite tuff map unit (Tbdt). Tdsr dikes gave U-Pb zircon ages of 51.2 ± 0.4 and 52.7 ± 0.3 Ma (AH21WW8, 23RL043, table 1).

Tr **Rhyolite (Tertiary: Eocene)**—Rhyolite dikes and sills containing potassium feldspar, plagioclase, quartz, and biotite phenocrysts in a quartz, plagioclase, and potassium feldspar groundmass. Orange to tan with coarse phenocrysts (up to 2.5 cm or 1 in). Heavily weathered. Rhyolite from Saddle Mountain has a U-Pb zircon age of 49.3 ± 0.2 Ma (23DS19, table 1). Neal and others (2023a,b) report a U-Pb zircon age of 51.8 ± 0.1 Ma for a Tr dike just off the north edge of the map.

Td **Dacite (Tertiary: Eocene)**—Light gray to tan porphyritic dacite dikes in the northwestern part of map. Groundmass is aphanitic. Phenocrysts of plagioclase, potassium feldspar, quartz, and biotite are common; hornblende is rare. Quartz phenocrysts are commonly rounded. U-Pb ages range from approximately 40 to 53 Ma (table 1, Howlett and others, 2020).

Tdu **Dikes, unknown (Tertiary: Eocene)**—Dikes with unknown composition, probably rhyolite or dacite. Forms ridges visible in lidar hillshade models and/or aerial photographs.

Tgd **Granodiorite (Paleocene–Eocene)**

Warren Lake Pluton—Variably porphyritic, medium- to fine-grained, equigranular biotite granodiorite with minor hornblende. Exposed along the north edge of the map. Non-foliated to weakly foliated. Wallace and others (1992) divided Tgd into the Warren Lake (TKw) and Maloney Basin (TKm) stocks. Mapped as TKgd by Ruppel and others (1993) and Lonn and others (2003), and Pggd by Neal and others (2023), who obtained a U-Pb zircon age of 51.9 ± 0.11 Ma.

Painted Rocks Pluton—Biotite granodiorite on the west-central edge of Wisdom 30' x 60' quadrangle. The Painted Rocks Pluton west of the quadrangle is described as having four phases, including altered pink, coarse-grained syenogranite; gray, medium-grained monzogranite; coarse-grained, porphyritic monzogranite with gray, euhedral, orthoclase phenocrysts; and granitic granophyre near the roof pluton (Lund and others, 1983; Berg and Lonn, 1996). Lund and others (1983) report K-Ar ages ranging from 50 to 40 Ma, and Daniels and Berg (1981) report a $^{40}Ar/^{39}Ar$ biotite age of 50.7 ± 2.1 Ma and a hornblende age of 52 ± 2.6 Ma. The Painted Rocks Pluton is intruded by dikes of the East Fork Dike Swarm (map units Tdsr and Tds) and is therefore older than approximately 52 Ma.

Tgb **Monzogranite, biotite (Eocene)**

Beaverhead Mountain Pluton—Located along the north edge of the map area. Described by Neal and others (2023a,b) as porphyritic, non-foliated biotite monzogranite with coarse quartz, orthoclase perthite, plagioclase, and microcline in a medium-grained plagioclase and quartz-rich groundmass. Subhedral orthoclase phenocrysts are up to 2.5 cm (1 in) long. Plagioclase phenocrysts have considerable sericitic alteration. Neal and others (2023a,b) report a U-Pb zircon age of 48.9 ± 0.1 Ma.

Tqs **Quartz syenite (Eocene)**—Single, large, coarse-grained equigranular to porphyritic dike in the west part of the map. The Saddle Mountain quartz syenite of Desmarais (1983), who

described the rock as primarily perthitic potassium feldspar (approximately 75 percent) with approximately 15 percent plagioclase, approximately 7 percent quartz, and lesser amounts of amphibole, biotite, pyroxene (aegirine/aegirine–augite), and opaque oxides that include magnetite cubes up to 0.5 mm. U-Pb zircon age is 49.3 ± 0.2 Ma (AH21WW3, table 1).

Tgbm **Granite, biotite–muscovite (Paleocene–Eocene)**—Fine- to coarse-grained, porphyritic, biotite–muscovite granite and granodiorite plutons. A small unnamed Tgbm body within the Foolhen Pluton has a U-Pb zircon age of 62.8 ± 1.0 Ma (CE19PH11a, table 1).

Burnt Ridge Pluton—White, medium- to coarse-grained two-mica granodiorite that weathers to light pink in outcrop. Not foliated. Toth (1983, 1987) describes the granodiorite as containing 35–40 percent euhedral to anhedral quartz, 40–45 percent oligoclase ($An_{28–30}$), 20 percent microcline, and 3–5 percent biotite and muscovite. U-Pb zircon age is 62.8 ± 0.6 Ma (AH21WW12, table 1).

Trail Creek and Pintler Creek Pluton—Fine- to medium-grained two-mica granite, dacite, and granodiorite. Generally porphyritic, with matrix grain size ranging between fine and very coarse. Commonly associated with pegmatite and aplite dikes and sills. It is part of the Chief Joseph Complex. Makes up a large volume of the ADZ footwall and contains shear fabrics and mylonite that increase towards the detachment.

Howlett and others (2020) report U-Pb zircon ages of 65.4 ± 3.9 Ma and 60.9 ± 0.6 Ma for this unit near Pintler Lake. A U-Pb zircon age of 63.3 ± 0.6 Ma was obtained for a sample taken along Trail Creek as part of this study (CE20BHB15, table 1). Foster and others (2010) report $^{40}Ar/^{39}Ar$ cooling ages between 41 and 39 for Tgbm. Wallace and others (1992) report K-Ar ages between 54 and 49 Ma.

Rye Creek Pluton—Medium-grained, white to grayish, non-foliated to weakly foliated, equigranular biotite–muscovite granodiorite with leucocratic phases in the northwest corner of the map area. Contacts are intricately interfingered with older igneous phases and contain gneissic and mafic xenoliths and large (>10 cm, 4 in) feldspar xenocrysts. U-Pb zircon age is 64.4 ± 0.8 Ma (AH21WW10, table 1).

TKdi **Diorite (Late Cretaceous–Paleocene)**—Dense, medium-grained, equigranular mafic rock with plagioclase, hornblende, pyroxene, and minor quartz visible in hand sample. Dikes occur in proximity to and along the Lick Creek fault and are possibly equivalent to a mafic dike (Yim) along Anderson Creek in the southeast corner of the map. A sample taken for U-Pb dating yielded no zircons. Several dikes have been prospected.

TKg **Granite (Late Cretaceous–Paleocene)**

Clifford Creek Pluton—Massive, light gray, coarse biotite–muscovite granite and porphyritic granite. Coarse granite is uniformly textured without obvious foliation, except locally where it is defined by biotite alignment. Muscovite forms euhedral intergrowths with biotite and also occurs as rare, large to small single crystals and alteration products. Porphyritic phase has white euhedral potassium feldspar phenocrysts as much as 3 cm long (Pearson and Zen, 1985). Zen (1988) reported K-Ar ages on biotite of 64.9 ± 2.2 Ma to 64.6 ± 2.1 Ma, and a $^{40}Ar/^{39}Ar$ age of 65.6 ± 1.4 Ma, and Roe (2010) reported a U-Pb zircon age of 71.3 ± 5.4 Ma.

Doolittle Creek Pluton—Fine-grained potassium feldspar–plagioclase–biotite ± muscovite granite and granodiorite densely intruded by aplite dikes and sills and associated milky quartz veins. Generally porphyritic, non-foliated to weakly foliated. Is described as biotite granite to granodiorite by Berger and others (1983a,b) but included in a biotite–muscovite granite suite by Ruppel and others (1993). Snee (1982) includes it in a "Late Group" of biotite granodiorite and tonalite plutons of the Pioneer Batholith. Snee (1982) reports a $^{40}Ar/^{39}Ar$ muscovite cooling age of 63.9 ± 0.8 Ma and a $^{40}Ar/^{39}Ar$ biotite cooling age of 61.3 ± 0.6 Ma. U-Pb zircon analysis yields an age of 68.2 ± 0.08 Ma (CE19PH7, table 1).

TKa **Aplite and pegmatite (Late Cretaceous or Paleocene)**—Tan, fine-grained, equigranular

silicic sills and associated smaller masses of alaskite and pegmatite that cut foliated Cretaceous granodiorite (Kgdf) and older rocks. The pegmatite consists mainly of potassium feldspar and smoky quartz crystals. A dike in TKYhcs near Mussigbrod Lake has a U-Pb zircon age of 63.3 ± 0.7 Ma (CE20BP4, table 1, fig. 10).

Mesozoic and Paleozoic Rocks

Kg **Granite (Late Cretaceous)**—Biotite granite to granodiorite plutons.

Grayling Lake Pluton—Medium- to coarse-grained, pinkish gray granite to granodiorite with 1 cm euhedral potassium feldspar phenocrysts in a matrix of white plagioclase, smoky-lilac quartz, biotite, and rare hornblende. Local foliation is defined by the alignment of biotite and feldspar. Sharp chilled margin. Reported K-Ar ages are 72 Ma (Zen, 1988) and 74 Ma (Marvin and others, 1983). Murphy and others (2002) report a U-Pb zircon age of 72.2 ± 1.7 Ma.

Francis Creek Pluton—White to gray, fine- to coarse-grained biotite granite to granodiorite with trace muscovite. Locally porphyritic. Not foliated. Intrudes granodiorite of Stewart Mountain Pluton. Related to the Grayling Lake Pluton (Zen, 1988). A U-Pb zircon age of 73.3 ± 0.6 Ma (KCS2136, table 1) was calculated for the body of the Francis Creek Pluton. A biotite granite sill within Yq near the pluton has a U-Pb zircon age of 72.9 ± 0.4 (KCS2134, table 1).

Stine Creek Pluton—Medium-grained, gray biotite ± muscovite granite to granodiorite. Muscovite only visible in thin section (Marvin and others, 1983). Secondary epidote and anhedral sphene (Zen, 1988). West end cuts Kgdf. Berger and others (1983) describe the pluton as an even-grained biotite ± hornblende granodiorite with local muscovite. K-Ar biotite ages for this unit are 72.3 ± 2.6 and 66.8 ± 2.4 Ma (Marvin and others, 1983). U-Pb zircon age of 74.6 ± 0.8 Ma (KCS2111, table 1).

French Basin Pluton—Biotite granite to granodiorite in the northwest corner of the map area. Granite/granodiorite is medium- to coarse-grained and porphyritic with phenocrysts up to 5 cm (1.5 in) of orthoclase and plagioclase (Desmarais, 1983). Orthogneiss is composed of alternating biotite-rich and quartz–feldspar-rich layers up to 6 cm (2 in) thick and contorted into isoclinal and ptygmatic folds.

Kgd **Granodiorite (Cretaceous)**—Primarily non-foliated biotite–hornblende granodiorite to tonalite. Includes non-foliated zones within the Foolhen Mountain Pluton and part of the Uphill Creek Pluton. A biotite-rich, non-foliated zone of Kgd from within Foolhen Complex Kgdf yielded a U-Pb zircon age of 73.9 ± 0.4 Ma (CE18FH14, table 1).

Dodgson Creek Pluton—Mostly gray, medium-grained, slightly porphyritic, hornblende–biotite granodiorite and quartz monzonite. Locally foliated. A sample from the eastern part of the map yielded K-Ar ages of 76.4 ± 2.6 Ma (biotite) and 95.9 ± 2.8 and 98.8 ± 2.8 Ma (hornblende; Marvin and others, 1983). Marvin and others (1983) also determined fission track ages of 72.4 ± 4.4 Ma (sphene) and 61.8 ± 9.1 Ma (zircon). Snee (1982) classified the pluton as "pre-main stage" and obtained hornblende and biotite $^{40}Ar/^{39}Ar$ ages ranging from 92 to 75 Ma. U-Pb zircon age of 76.1 ± 0.3 Ma was obtained in this study (CE23W100K08, table 1). Kgtd of Ruppel and others (1993).

Proposal Rock Pluton—Pinkish gray, medium- to coarse-grained, porphyritic, biotite granodiorite and granite. Non-foliated to weakly foliated. Snee (1982) and Berger and others (1983) classified the pluton as late-stage and grouped it with the Shoestring Creek Pluton. Ruppel and others (1993) mapped it as Kgbb biotite granite and granodiorite, and related it to the Grayling Lake Pluton. $^{40}Ar/^{39}Ar$ ages range from 71 to 67 Ma (Shoestring Pluton of Snee, 1982). U-Pb zircon analysis yields an age of 68.4 ± 0.5 Ma (CE19PH1, table 1).

Mono Park Pluton—Gray medium-grained porphyritic biotite granodiorite with minor hornblende. Has phenocrysts of potassium feldspar up to 6 cm (2 in) long. May grade into the

Uphill Creek Pluton (Lonn, 2015). Is mapped as Kbgg by Ruppel and others (1993) and Kgdp by Lonn and others (2019). U-Pb zircon age is 70.1 ± 0.4 Ma (KCS2019, table 1).

Kgdb **Granodiorite, biotite (Late Cretaceous)**—Pale pink to pinkish gray granodiorite of the **Odell Lake Pluton** with phenocrysts of plagioclase, potassium feldspar, and 5 percent biotite. Hornblende is locally abundant. Forms a small body near Odell Lake in the center of the map. The Odell Lake Pluton yielded a U-Pb zircon age of 68.7 ± 0.5 (KCS2004, table 1) and a $^{40}Ar/^{39}Ar$ biotite age 66.0 ± 0.7 Ma (Snee, 1982).

Kgdf **Granodiorite, foliated (Late Cretaceous)**

Foolhen Pluton—Gray, medium- to coarse-grained granular to porphyritic granodiorite and tonalite (Elliott and Lonn, 2021). Contains 5–35 percent biotite, hornblende, or biotite and hornblende, and 5–56 percent potassium feldspar (Truckle, 1988). Hornblende increases in abundance towards the south and west. Mafic inclusions abundant. Varies from massive to weakly foliated (preferred dimensional orientation fabric), to strongly gneissic, particularly near contacts with Kqsg. At Chalk Bluff, Kgdf is massive at the bottom of the hill but grades to strongly gneissic at the contact with Kgn metasedimentary rocks. The contact is not parallel to gneissosity, suggesting that it is tightly folded and that the compositional layering is axial planar to the folds. Alternately, it is possible that the metasedimentary rocks and granodiorite were interleaved before deformation. Includes light gray, fine-grained aplite dikes with up to 15 percent plagioclase and 5 percent biotite. Also contains metasedimentary xenoliths of all sizes, from hand sample to map scale. U-Pb zircon ages for foliated samples of the Foolhen Pluton are 73.7 ± 0.3 and 72.5 ± 0.5 Ma (KCS2112, CE19FH1, table 1), which overlap with that of the nonfoliated sample mentioned above under Kgd. Foster and others (2012) obtained a zircon U-Pb age of 72.5 ± 3 Ma and Roe (2010) obtained a U-Pb zircon age of 71.8 ± 2.0 Ma for samples from Chalk Bluff.

Stewart Mountain Pluton—Gray, medium- to coarse-grained granodiorite, similar to the Foolhen Complex. It varies from massive to weakly foliated and contains biotite and/or hornblende. The Stewart Mountain Pluton yielded a U-Pb zircon age of 71.8 ± 0.5 Ma (KCS2012, table 1).

Martin Creek Pluton—Gray, medium-grained, equigranular biotite–hornblende granodiorite locally varying to tonalite and quartz–diorite. Mostly non-porphyritic. Foliation ranges between weak and intense, defined by the preferred orientation of biotite and hornblende, with zones of gneissic compositional layering. Foliation increases towards the edges of the pluton. Desmarais (1983) reports a zone of orbicular texture along the northern border of the pluton. U-Pb zircon age is 72.3 ± 0.4 Ma (AH21WW9, table 1).

Kgdp **Porphyritic granodiorite (Late Cretaceous)**—Gray, porphyritic, medium- to coarse-grained biotite–hornblende granodiorite of the **Uphill Creek Pluton**. Characterized by anhedral megacrysts of potassium feldspar with inclusions of other minerals. This constitutes the largest pluton of the Pioneer Batholith. Flow foliation, defined by the alignment of mafic minerals, is poorly to moderately developed. U-Pb zircon ages are 68.2 ± 0.3, 70.7 ± 0.5, and 70.9 ± 0.4 Ma (KCS2110, KCS2129, KCS2130, table 1). Snee (1982) reports an Ar^{40}/Ar^{39} date of 75 Ma and has published U-Pb zircon ages of 72.2 ± 0.6 Ma (Murphy and others, 2002) and 72.0 ± 0.5 (Foster and others, 2012). Also includes light gray, massive, medium-grained hornblende–biotite granodiorite (Kgd; Pearson and Zen, 1985; Zimbelman, 1984).

Kgn **Gneiss of Foolhen Ridge (Late Cretaceous)**—Quartz–feldspar–biotite–hornblende gneiss that reflects a granitic protolith mixed with quartz–feldspar–biotite–cordierite metasedimentary gneiss. Typically gray, very fine-grained, and intensely foliated, with mylonitic zones and evidence of transposition. Locally strongly lineated. Elliott and Lonn (2021) obtained a zircon age of 73.3 ± 0.4 Ma (sample CE18FH13a). Metasedimentary protoliths are

uncertain and could be any age from Mesoproterozoic to Mesozoic. Kgn is equivalent to Xm of Berger and others (1983), who interpreted the unit to be Paleoproterozoic basement gneiss. Ruppel and others (1993) reinterpreted the unit as metamorphosed Cretaceous igneous rock.

KMsm **Metasedimentary rocks (Mississippian through Cretaceous, Cretaceous metamorphic age)**—Layered, folded, severely deformed rock with rare recognizable primary structures. Includes metamorphosed sandstone, conglomerate, and quartzite. Truckle (1988) mapped these as formations in the regional Phanerozoic stratigraphic framework, but our mapping suggests that while Phanerozoic protoliths are possibly identifiable in some cases (e.g., dense, purple quartzite with apatite nodules might be metamorphosed Phosphoria Formation), stratigraphic relationships are not retained. Messenger (2016) interpreted the protolith of the carbonates that host the Calvert tungsten deposit as Pennsylvanian. We interpret KMsm to be in fault contact with Yqsg and intruded by Kgdf.

Kbl **Blackleaf Formation (Cretaceous)**—Poorly exposed, medium gray to dark gray mudstone, shale, and siltstone, locally slaty or phyllitic. Shale is fissile, often carbonaceous or bioturbated. Mudstone and shale are underlain by, and interbedded in the lower portion with, gray to yellow brown calcareous siltstone; tan to gray, fine-grained calcareous sandstone; and gray to brown, fine-crystalline limestone. Up to 760 m (2,500 ft) thick in the east adjacent Butte South 30' x 60' quadrangle (McDonald and others, 2012).

Kk **Kootenai Formation (Cretaceous)**— Folded and foliated slate, metasandstone, and metaconglomerate with blobs and layers of marble. Metaclastic rocks are shades of gray and green with maroon and black lenses. Relict fossils in the marble identify it as the gastropod limestone that regionally caps the Kootenai Formation. Late Cretaceous metamorphic age. Thickness not determined.

Trd **Dinwoody Formation (Triassic)—** Poorly exposed yellowish gray, grayish brown, and pale red, thin-bedded limestone, siltstone, and shale. Siltstone and shale are locally calcareous. Occurs in small exposures along the eastern edge of the map sheet. Thickness in the east-adjacent Wise River 7.5' quadrangle is 170 m (550 ft; Fraser and Waldrop, 1972).

Pzs **Paleozoic sedimentary rocks, undivided (Paleozoic)**—Sheared and brecciated light gray limestone and dolomite. It occurs in two small fault slices along the Ross Gulch and Pettengill faults near the east central edge of the map.

Pq **Quadrant Formation (Pennsylvanian)**—Light gray, fine- to medium-grained, quartzitic sandstone and vitreous quartzite. Weathers light yellow brown to pale reddish brown, forms resistant ridges and isolated knobs. Bedding is rarely visible. Commonly brecciated. Thickness unknown.

PMsr **Snowcrest Range Group (Mississippian and Pennsylvanian)**—Poorly exposed, grayish red mudstone and siltstone, grayish yellow to grayish orange calcareous fine-grained sandstone, medium gray to light olive-gray limestone and reddish orange limestone solution breccias. Sandstones are thinly bedded. Small yellow reduction spots are common in red siltstones, which characterize the upper portion of the unit; limestones and calcareous sandstones are more common in the lower portion. Equivalent to Amsden Formation. Thickness unknown.

PMs **Snowcrest Range Group and Quadrant Formation, undifferentiated (Paleozoic: Mississippian and Pennsylvanian)**—Thin thrust sliver of clean quartzite and deformed limestone near the east edge of the map, north of center. Thickness unknown.

Mm **Madison Group limestone (Mississippian)**—Thickly bedded limestone exposed in a small area above the Johnson thrust on the east edge of the map. Mm appears to be the protolith of a tectonic breccia of white carbonate that forms a small but remarkable spire in the northern part of the map. Clasts are angular, millimeters to decimeters across, calcite cemented. Thickness unknown.

Dj **Jefferson Formation (Devonian)**—Dark gray, yellow, and white, sugary dolomite and limestone, commonly bleached and recrystallized to white marble. Dark gray dolomite distinguishes this unit from the Hasmark Formation (unit Ꞓh). Strongly deformed, with numerous intraformational faults, abundant tectonic breccia, and tight folds. Deformation makes thickness estimates problematic, but probably more than 300 m (1,000 ft) thick.

Ꞓsm **Metamorphosed sedimentary rocks, undivided (Cambrian protolith, Cretaceous metamorphism)**—Along the north edge of the map area, Ꞓsm is fine- to coarse-grained, well-sorted quartzite that contains well-rounded grains of 98–100 percent quartz of the Flathead Formation, grading up to phyllite, marble, and calc-silicate gneiss with wavy laminae of the Silver Hill Formation, and then up to massive, bluish gray dolomite of the Hasmark Formation that commonly displays mottled weathering. In the eastern edge of the map area, Ꞓsm is laminated, grayish green to dark gray phyllite, argillite, and siltite, interbedded with vitreous quartzite and greenish calc-silicate laminae, and white to purple, medium- to coarse-grained, well-sorted quartzite. Commonly massive but locally contains heavy mineral layer laminae that define beds and crossbeds (Lonn and McDonald, 2004b). Ꞓsm correlates with the Swamp Creek sequence of Zen (1988) exposed in the east-adjacent Butte South 30' x 60' quadrangle (McDonald and others, 2012), which is thought to be the metamorphosed equivalent of the Silver Hill Formation (Lonn and McDonald, 2004b). Thickness unknown.

Ꞓrlh **Red Lion and Hazmark Formations, undivided (Paleozoic: Cambrian)**—Light gray to white, thinly laminated to massive dolomite with minor magnesium limestone intervals. Light gray with a smooth, laminated surface. Locally includes the lower part of the Red Lion Formation, a lithologically variable unit that includes red dolomite with thin maroon anastomosing shale layers, shaly conglomerate containing limestone and mud-chip intraclasts, reddish calcareous silty shale, and calcareous to non-calcareous sandstone and quartzite. Thickness variable due to deformation, ranging from 200–500 m (650–1,640 ft).

Ꞓglq **Quartzite of Grace Lake (Paleozoic: Cambrian)**—White to light gray, fine- to medium-grained quartzite. Contains coarse intervals with rounded quartzite pebbles and angular grains of quartzite, quartz, and feldspar; some beds of coarse sand. Lacks the pink and red quartzite and brick-red chert clasts of the Black Lion Formation (unit Ybl). Grains are subrounded to subangular, and moderately to well-sorted, although coarse intervals are poorly sorted. Contains abundant well-rounded quartz grains. In hand sample, the finer-grained intervals appear feldspar-poor, but slabbed and stained samples contained 15–25 percent K-spar and 5–10 percent plagioclase. Flat laminations are common, as are trough crossbeds in the coarse intervals. Base is exposed at Grace Lake southeast of the map, where a low-angle unconformity with the underlying Black Lion Formation is clearly visible (McDonald and others, 2012). Appears to grade upward into the quartzite and argillite of unit Ꞓsh at Grace Lake. Equivalent to the quartzite of Grace Lake of Ruppel and others (1993), and the Cambrian or Proterozoic quartzite of Pearson and Zen (1985). Thickness unknown but at least 75 m (244 ft) exposed at Grace Lake east of the quadrangle. The only exposure on the Wisdom quadrangle is along the eastern edge of the map.

ꞒYq **Quartzite, undivided (Mesoproterozoic to Cambrian)**—Purple to light gray, dense, fine- to medium-grained, feldspar-poor, massive quartzite that contains sparse floating pebbles of quartz, interbedded with and grading downward into fine- to coarse-grained feldspathic quartzite with abundant mud chips, trough and planar crossbeds, and flat laminations. The fine-grained quartzite has a flinty fracture and is micaceous and strongly foliated. Some of the feldspathic quartzite contains granule-sized grains and pebbles of quartz and quartzite. Slabbed and stained samples of this unit show feldspar content of 1–27 percent, with potassium feldspar content being much greater than plagioclase content. Because this unit was observed in apparent depositional contact with

Cambrian sediments, this unit is thought to include a Cambrian-age quartzite and Mesoproterozoic Lemhi subbasin quartzite. Thickness unknown.

Precambrian Rocks

ZYdi **Diorite (Proterozoic)**—Dark gray altered dikes containing olivine and/or augite, lath-shaped feldspar, pyroxene, and opaque minerals (Zen, 1988). Intrudes the Lambrecht Creek fault in the southeastern part of the map and also occurs as sills in this area.

Yim **Intrusive rock, mafic** (Mesoproterozoic)—Fine- to medium-grained mafic dike in the southwest part of the quadrangle. White plagioclase as much as 30 percent. Original hornblende and pyroxene partly altered to amphibole, chlorite, and epidote, likely during late Cretaceous metamorphism. Appears to have intruded along, and was subsequently cut by, the Anderson Creek fault. U-Pb zircon analysis (23RB406, table 1) yielded a $^{207}Pb/^{206}Pb$ weighted mean age of 1,264 ± 15 Ma. One concordant (likely inherited) grain yielded an approximate age of 1,747 Ma and one discordant grain showed Cretaceous or younger Pb-loss.

Ybl **Black Lion Formation (Mesoproterozoic?)**—Pink, green, and purple conglomerate containing abundant multi-colored lithic fragments. Prominently crossbedded, with both trough and high-angle planar crossbeds. Composition is highly variable, reflecting local source areas. Abundant gritty intervals containing angular gneissic, granitic, and dark-colored lithic clasts. Contains distinctive brick-red laminated chert (siltstone?) and pink to purple quartzite clasts that are usually rounded; these clasts are rare to absent in the overlying Grace Lake quartzite (map unit Ꞓglq). The upper contact is an angular unconformity with Ꞓglq, well-exposed in the Grace Lake area on the east adjacent Butte South 30’ x 60’ quadrangle (McDonald and others, 2012), and very poorly exposed along the east edge of this map. The lower contact appears to be an unconformable contact with the underlying gneiss (Xgn) on the east-adjacent Butte South 30’ x 60’ quadrangle (McDonald and others, 2012). Interpreted to be a Belt basin marginal deposit similar to the LaHood Formation of the Highland Mountains, but younger, of upper Belt age, based on intervals of similar lithology within the Swauger Formation near the eastern border of the map. As much as 500 m (1,625 ft) thick.

Yqsg **Quartzite, schist, gneiss, and migmatite (Mesoproterozoic protolith, Cretaceous metamorphic age)**—Fine- to medium-grained amphibolite-facies quartz-potassium feldspar-plagioclase-muscovite-biotite±sillimanite±garnet metasedimentary gneiss, quartzite, and schist that is commonly migmatitic (fig. 11). Migmatite neosome is fine- to medium-grained biotite-muscovite granite locally injected or segregated in foliation-parallel sheets (lit-par-lit), as blobs in fold hinges, or parallel to the axial plane of folds.

Figure 11. Unit Yqsg quartzite, schist, gneiss, and migmatite in the Foolhen Complex. (A) Identifiable quartzite (light) and metapelite (dark) layers that might be bedding. Note the large muscovite flakes in the metapelite.(B) Yqsg metasediments intermixed with granitic melt, indicating a complex relationship among deformation, metamorphism, and intrusion. The dashed line follows a sharp length of boundary between metasediment and partial melt. The borders between the two are commonly more diffuse.

Yqsg is intensely deformed, with several fold generations. Gneissosity shown on map is mostly a transposition foliation and is the most recent fabric.

Mapped by Truckle (1988) and Berger and others (1983) as Paleoproterozoic metamorphic rock, but by Ruppel and others (1993) as metamorphosed Mesoproterozoic Belt Supergroup. Three samples of Yqsg produced detrital zircon spectra consistent with a Belt-aged protolith (CE16FH1, CE18FH9, Elliott and Lonn, 2021; CE19PH4, table 1). Samples CE16FH1 and CE18FH9 each yielded a single concordant igneous zircon aged 73 Ma, pointing to a Cretaceous metamorphic age (table 1). Locally, Yqsg grades into less metamorphosed, recognizable Belt units (Ysw and Ylc), but most often its stratigraphic position cannot be determined.

Ymi **Missoula Group and Lemhi subbasin strata (Mesoproterozoic)**—Light gray, fine- to coarse-grained, poorly sorted, feldspathic quartzite containing rare floating pebbles and granules. Beds up to 1 m (3 ft) thick commonly contain flat laminations, planar crossbeds, and/or trough crossbeds defined by black heavy mineral laminations. Lower contact is gradational with the underlying Piegan Group map unit (Ypn), upper contact not exposed. Lacks recognizable Snowslip and Shepard Formations of the lower Missoula Group, and is therefore thought to be part of the correlative Lemhi subbasin strata. The upper part includes intervals of thin-bedded quartzite and argillite. Thickness unknown, but at least 1,000 m (3,300 ft).

Ymim **Metamorphosed Missoula Group and Lemhi subbasin strata (Mesoproterozoic protolith, Cretaceous metamorphism)**—Light gray, fine- to coarse-grained, poorly sorted, feldspathic metaquartzite containing uncommon floating pebbles and granules. Feldspar content averages 20–25 percent. Strained zones or layers alternate with unstrained layers. Strongly foliated zones contain grains flattened in a plane roughly parallel to bedding. Unstrained zones contain flat laminations and large trough and planar crossbeds. Lower contact is the Sawed Cabin detachment fault; upper contact with overlying Ɛsm is a strongly foliated, ductilely strained zone. Thickness unknown, but at least 600 m (2,000 ft).

Yaj **Jahnke Lake member of the Apple Creek Formation (Mesoproterozoic)**—Pale gray to green, fine- to very fine-grained, plagioclase-rich quartzite. Locally, it has a pinkish cast where iron oxide is hematite. Beds are typically decimeter-scale with ripples, climbing ripples, load casts, and trough and planar crossbedding (Stewart and others, 2014). Locally, quartzite contains argillite as irregular chunks and flakes. Thickness unknown due to lack of upper contact but as much as 5 km (3 mi) thick in the south-adjacent Salmon 30' x 60' quadrangle (Lonn and others, 2019). Unit assignment based on stratigraphic position above the Lawson Creek Formation.

Ylca **Lawson Creek and Apple Creek Formations, undivided (Mesoproterozoic)**—Dominantly gray, flat laminated, very fine- to fine-grained quartzite in decimeter- to meter-thick beds separated by thin argillite skins. Convolute bedding, climbing ripple cross-laminations, and mud rip-up clasts are common. Contains uncommon beds up to 0.2 m (8 in) thick of feldspar-poor, medium-grained quartzite with abundant well-rounded spherical grains. Contains intervals as much as 100 m (33 ft) thick dominated by centimeter-scale siltite–argillite couplets with abundant mud rip-ups, desiccation cracks, load casts, and centimeter-scale lenses of feldspar-poor, medium-grained quartzite. Also contains rare calc-silicate intervals as much as a meter thick, black argillite beds as much as 20 cm (8 in) thick, and millimeter-scale siltite–argillite microcouplets. Tentatively correlated with the Lawson Creek Formation and overlying Apple Creek Formation of the Lemhi subbasin (Burmester and others, 2016). Equivalent to the Sequence of Big Point of Zen (1988). At least 1,000 m (3,300 ft) exposed.

Ylc **Lawson Creek Formation (Mesoproterozoic)**—Characterized by couplets (centimeter-scale) and couples (decimeter-scale) of fine- to medium-grained white to pink quartzite and

red, purple, black, and green argillite. Lenticular and flaser bedding are common and characteristic. Mud rip-up clasts are locally common, and some are as much as 15 cm (6 in) in diameter. Thick intervals of medium-grained, thick-bedded (meter-scale) quartzite are commonly interbedded with the argillite-rich intervals. The quartzite intervals appear similar to the upper part of the underlying Swauger Formation (unit Ysw), but quartz typically comprises a large percentage of the grains (up to 93 percent) in contrast to the feldspathic Swauger Formation. Except in the uppermost part, potassium feldspar is more abundant than plagioclase. In the eastern part of the map area, the lower contact is exposed and is placed at the bottom of the thin-bedded argillite-rich interval that gradationally overlies the Swauger Formation. A complete stratigraphic section is only exposed in the southwestern part of the map, where it is less than 300 m (1,000 ft) thick (Stewart and others, 2014), but an incomplete section in the southeastern part of the map is least 900 m (3000 ft) thick.

Ysw **Swauger Formation (Mesoproterozoic)**—Light gray, poorly sorted, fine- to coarse-grained feldspathic quartzite and pebble conglomerate. Bed thicknesses range from 0.2 to 1.0 m (8 in to 1 ft). Contains obvious chalky white feldspar grains, large trough crossbeds, detrital muscovite, and metamorphic (?) biotite along bedding planes. Lenses and intervals of conglomerate have round pebbles up to 2 cm (0.8 in) of fine-grained quartzite and angular granules and small pebbles of feldspar and quartz, suggesting at least two source areas. Rare thin argillite beds/skins typically contain desiccation cracks. Feldspar content variable, but samples slabbed and stained reveal more potassium feldspar than plagioclase. The coarse grains, high potassium feldspar content relative to plagioclase, and thick stratigraphic section correlate with the Swauger Formation of the Lemhi subbasin strata, upper Belt Supergroup (Burmester and others, 2016). Thickness at least 1,600 m (5,300 ft) thick. Unit is equivalent to pCm2 and pCm3 of Truckle (1988) and Ym of Ruppel and others (1993).

Ygs **Gunsight Formation (Mesoproterozoic)—** Quartzite, siltite, and minor argillite mapped in the southwestern corner of the map. Stewart and others (2014) described it as gray, gray-green, and tan, well-sorted, fine-grained, feldspar-rich quartzite. Features include abundant heavy mineral laminations and soft-sediment deformation. The quartzite is well sorted, and is laminated to thinly bedded, commonly showing ripples, climbing ripples, load casts, and trough and planar crossbedding. Upper contact gradational above approximately 400 m (1,300 ft) of green to light gray, siltite to fine-grained quartzite (Stewart and others, 2014). Thickness on the map uncertain but estimated to be approximately 4,500 m (15,000 ft; Stewart and others, 2014). Stratigraphic position under the Swauger Formation supports assigning this unit to the Gunsight Formation, the highest unit of the Lemhi Group.

Yqcs **Quartzite and calcsilicate (Mesoproterozoic)**—Quartzite, siltite, calc-silicate rocks, and minor schist and phyllite. Bedding on centimeter to decimeter scale. Near the west edge of the map, the abundance of calc-silicate rocks decreases northward, which is interpreted to be downsection. Includes phyllite, schist, and gneiss near contacts with plutonic rocks. Calc-silicate rocks are resistant to weathering and commonly crop out. They contain abundant actinolite along with plagioclase and local scapolite. Thickness is unknown as the lower and upper stratigraphic contacts were not found; the minimum thickness is 1,000 m (3,300 ft). Previously mapped as calc-silicate, quartzite, and siltite of Dahlonega Creek (Stewart and others, 2014). If stratigraphically below the Gunsight Formation (Ygs), lithologies correlate with the Yellow Lake Formation, which contains carbonate, and possibly parts of the Big Creek Formation, predominantly very fine-grained quartzite and siltite, both of the Lemhi Group (Burmester and others, 2016). Alternatively, the unit is correlative to the Apple Creek–Lawson Creek Formations unit (Ylca) mapped in the eastern part of the Wisdom quad. However, Yqcs lacks the diagnostic thin beds of rounded, medium-grained quartz present in Ylca.

Ysh **Shepard Formation (Mesoproterozoic)**—Distinguished by dark green siltite and light green argillite in microlaminae and couplets that are dolomitic and have a characteristic orange-brown-weathering rind. The upper part is red, thinly bedded dolomitic quartzite and siltite. Poorly exposed, but weathers into thin plates. Estimated to be 152 m (500 ft) thick.

Ysn **Snowslip Formation (Mesoproterozoic)**—Mostly thin-bedded green or gray sand to clay couplets with abundant ripples, mud rip-up clasts, and mud cracks. Green and dark gray, dolomitic, siltite–argillite laminae are common near the base. Increasing amounts of siltite and quartzite occur upsection. Includes rare thin lenticular beds of coarse-grained quartzite that contain granule-sized lithic fragments. The upper portion is mostly flat-laminated, medium- to coarse-grained quartzite in beds 0.3–1 m (1–3 ft) thick and may be correlative with the part of the Gunsight Formation (Yg) mapped on the western part of the map. Thickness as much as 900 m (3,000 ft).

Ysnm **Metamorphosed Snowslip Formation (Mesoproterozoic protolith, Cretaceous metamorphism)**—Lower part is thinly laminated millimeter-scale phyllite and calc-silicate, and centimeter- to decimeter-scale interlayered schist and quartzite. Upper part is fine- to medium-grained, poorly sorted feldspathic quartzite in beds 0.3 to 1 m (1 to 3 ft) thick. It contains abundant flat laminations and climbing ripples, and uncommon trough crossbeds. Feldspar content averages 15–25 percent, with plagioclase predominant over potassium feldspar. Mapped in the north central part of the quadrangle. No complete stratigraphic section is exposed; the minimum thickness is 900 m (3,000 ft).

Ypn **Piegan Group (Mesoproterozoic)**—Thin-bedded tan-weathering calcitic and dolomitic siltite and quartzite that grade up to black argillite located in the north central part of the map. Pinch-and-swell bedding is on a centimeter to decimeter scale. Molar-tooth structure and non-polygonal "crinkle" cracks are common. The upper contact is gradational with overlying quartzite of Ymi; the lower contact is a fault. Only the uppermost part of the section is exposed. Thickness is approximately 1,200–1,800 m (4,000–6,000 ft; Lidke and Wallace, 1992; Wallace and others, 1992).

Ypnm **Metamorphosed Piegan Group (Mesoproterozoic protolith, Cretaceous metamorphism)**—Calc-silicate gneiss with decimeter- to centimeter-scale layers of dense, greenish, diopside-rich calc-silicate rock, very fine-grained quartzite, marble, dolomite, and minor schist. While some layers still exhibit original sedimentary structures, including graded centimeter-scale couplets of light brown siltite up to black argillite, others have developed a strong layering-parallel schistosity (S_1) and contain isoclines and sheath folds. Layers of marble and dolomite are common and diagnostic of this unit on the Wisdom quadrangle. Correlation with the Piegan Group of the Belt Supergroup is based on its gradation to less metamorphosed strata north of the quadrangle mapped as Piegan Group (Lonn and others, 2003); its lower gradational contact with metamorphosed Ravalli Group; and its upper gradational contact with metamorphosed Snowslip Formation. Thickness is variable due to deformation, but the original stratigraphic thickness was approximately 1,200–1,800 m (4,000–6,000 ft; Lidke and Wallace, 1992; Wallace and others, 1992).

Ypnm+Kgdf Areas where dikes and sills of Kgdf are as abundant as Yram.

Yram **Metamorphosed Ravalli Group (Mesoproterozoic protolith, Cretaceous metamorphism)**—Gray, fine- to medium-grained, strongly foliated quartzite beds 15 cm to 1.5 m (6 in to 5 ft) thick separated by thin phyllite or biotite–muscovite schist layers. Original sedimentary structures are sometimes preserved and include abundant flat laminations, trough crossbeds, and contorted bedding created by soft-sediment deformation. The upper stratigraphic contact is gradational with the metamorphosed Piegan Group, and the lower contact is gradational with the metamorphosed Prichard Formation. Thickness more than 1,200 m (4,000 ft).

Ypm **Metamorphosed Prichard Formation (Mesoproterozoic protolith, Cretaceous metamorphism)**—Quartz–feldspar–biotite–muscovite–garnet gneiss, schist, and phyllite. Contains intervals of calc-silicate gneiss with pale green centimeter-scale layers of fine-grained quartz with white and green amphiboles (actinolite + tremolite) ± calcite ± dolomite ± epidote ± wollastanite ± garnet, as well as millimeter to 20 centimeter-thick (0.04–8 in) layers of quartz–feldspar metasandstones and micaceous metashale. Layers are commonly discontinuous and contain rootless isoclines parallel to layering that represents transposition foliation (S_1), with two overprinting crenulation cleavages typically present. Some intervals preserve distinctive graded couplets of siltite up to black argillite and rusty weathering decimeter layers of silt. A thick overturned metamorphosed stratigraphic section exposed on the west face of West Goat Peak in the northwest corner of the map suggests that the protolith is the Prichard Formation stratigraphically below the Ravalli Group. Calc-silicate intervals are interpreted to represent the carbonate-bearing intervals found at the top of the Prichard Formation or in the Prichard Formation–Ravalli Group transition. The original upper stratigraphic contact is gradational with the overlying Ravalli Group. The lower stratigraphic contact is not preserved. The original stratigraphic thickness is unknown, but in the central Belt basin is at least 6,000 m (20,000 ft).

Ypm+Tgbm Areas where dikes and sills of Tgbm are as abundant as Ypm.

Xgn **Gneiss and amphibolite (Paleoproterozoic)**—Foliated plagioclase gneiss, augen gneiss, banded fine-grained and coarse-grained gneiss, and amphibolite. Foster and others (2006) interpreted a U-Pb age of 1.86 Ga to represent the crystallization age of the protolith. Only exposed in one small area on the east edge of the map.

ACKNOWLEDGMENTS

Reviews by Jo-Ann Sherwin, Idaho State University, Madeline Lewis, University of Wyoming, and Dan Brennan, Katie McDonald, Jesse Mosolf, Stuart Parker, and Steve Quane of the MBMG greatly enhanced this map and report, as did discussions with members of the Idaho Geological Survey, Reed Lewis in particular. We are grateful for everyone's contributions, but accept all errors as our own.

REFERENCES

Armstrong, R.L., and Ward, P., 1991, Evolving geographic patterns of Cenozoic magmatism in the North American Cordillera: The temporal and spatial association of magmatism and metamorphic core complexes: Journal of Geophysical Research: Solid Earth, v. 96, no. B8, p. 13201–13224, https://doi.org/10.1029/91JB00412

Badley, R.H., 1978, Petrography and chemistry of the east fork dike swarm, Ravalli County, Montana: Missoula, University of Montana, M.S. thesis, 54 p., available at https://scholarworks.umt.edu/etd/7726 [Accessed August 2025].

Bausch, W.G., 2013, Petrology, geochemistry, and age of extension in the lost trail pass dike swarm, southwest Montana: Missoula, University of Montana, M.S. thesis, 83 p., available at https://scholarworks.umt.edu/etd/1382 [Accessed August 2025].

Bausch, W.G., Baldwin, J.A., and Foster, D.A., 2013, Synextensional emplacement and cooling of the East Fork Dike Swarm at Lost Trail Pass, southwest Montana: Northwest Geology, v. 42, p. 299–308.

Berg, R.B., and Lonn, J.D., 1996, Preliminary geologic map of the Nez Perce Pass 30' x 60' quadrangle, Montana: Montana Bureau of Mines and Geology Open-File Report 339, 9 p., 1 sheet, scale 1:100,000.

Berger, B.R., Snee, L.W., and Hanna, W., 1983a, Mineral resource potential of the West Pioneer wilderness study area, Beaverhead County, Montana: U.S. Geological Survey Miscellaneous Field Studies Map MF-1585, scale 1:50,000, available at https://pubs.usgs.gov/mf/1983/1585a/plate-1.pdf [Accessed August 2025].

Berger, B.R., Snee, L.W., Hanna, W., and Benham, J.R., 1983b, Mineral resource potential of the West Pioneer Wilderness Study Area, Beaverhead County, Montana: U.S. Geological Survey Miscellaneous Field Studies Map MF-1585A, 21 p., https://doi.org/10.3133/mf1585A

Borradaile, G.J., Bayly, M.B., and Powell, C.M. eds., 2012, Atlas of deformational and metamorphic rock fabrics: Springer Science & Business Media, https://doi.org/10.1007/978-3-642-68432-6

Brennan, D.T., Parker, S.P., Mosolf, J.S., and Kylander-Clark, A., 2025, U-Pb geochronology data from rock samples collected in the Dillon, Polson and Wisdom 30′ x 60′ quadrangles, western Montana, 2023–-2024: Montana Bureau of Mines and Geology Analytical Dataset 16, https://doi.org/10.59691/TXET7641

Burmester, R.F., Lonn, J.D., Lewis, RS., and McFaddan, M.D., 2016, Stratigraphy of the Lemhi subbasin of the Belt Supergroup, *in* MacLean, J.S, and Sears, J.W., eds., Belt Basin: Window to Mesoproterozoic Earth: Geological Society of America Special Paper 522, p. 121–137, https://doi.org/ 10.1130/2016.2522(05)

Busby, C.J., Pavlis, T.L., Roeske, S.M., and Tikoff, B., 2023, The North American Cordillera during the Mesozoic to Paleogene: Selected questions and controversies, *in* Whitmeyer, S.J., Williams, M.L., Kellett, D.A., and Tikoff, B., eds., Laurentia: Turning points in the evolution of a continent: Geological Society of America Memoir 220, p. 635–658, https://doi.org/10.1130/2022.1220(31)

Calede, J.C., and Rasmussen, D.L., 2015, Field guide to the geology and paleontology of the cabbage patch beds of the Flint Creek Basin (Renova Formation, Arikareean): Northwest Geology, v. 44, p. 157–188.

Culshaw, N.G., Beaumont, C., and Jamieson, R.A., 2006, The orogenic superstructure–infrastructure concept: Revisited, quantified, and revived: Geology, v. 34, no. 9, p. 733–736, https://doi.org/10.1130/G22793.1

Daniel, F., and Berg, R.B., 1981, Radiometric dates of rocks in Montana: Montana Bureau of Mines and Geology Bulletin 114, 144 p., 2 sheets.

Desmarais, N.R., 1983, Geology and geochronology of the Chief Joseph plutonic–metamorphic complex, Idaho–Montana: Seattle, University of Washington, Ph.D. dissertation, 150 p., scale 1:50,000.

Dostal, J., and Jutras, P., 2022, Tectonic and petrogenetic settings of the Eocene Challis–Kamloops volcanic belt of western Canada and the northwestern United States: International Geology Review, v. 64, p. 2565–2583, https://doi.org/10.1080/00206814.2021.1992800

Dudás, F.Ö., Ispolatov, V.O., Harlan, S.S., and Snee, L.W., 2010, $^{40}Ar/^{39}Ar$ geochronology and geochemical reconnaissance of the Eocene Lowland Creek volcanic field, west-central Montana: Journal of Geology, v. 118, p. 295–304, https://doi.org/10.1086/651523

Elliott, C.G., 2015, Geologic map of the Lower Seymour Lake 7.5’ quadrangle, southwestern Montana: Montana Bureau of Mines and Geology Open-File Report 664, 11 p., 1 sheet, scale 1:24,000.

Elliott, C.G., 2017, Geologic map of the Lincoln Gulch 7.5' quadrangle, southwestern Montana: Montana Bureau of Mines and Geology Geologic Map 70, 1 sheet, scale 1:24,000.

Elliott, C.G., 2019, Multiphase extension in the hangingwall of the Anaconda Detachment Zone: Northwest Geology, v. 48, p. 71–82.

Elliott, C.G., 2022, Geologic map of the Pine Hill 7.5' quadrangle, southwest Montana: Montana Bureau of Mines and Geology Geologic Map 87, 1 sheet, scale 1:24,000, https://doi.org/10.59691/UKJI1478

Elliott, C.G., 2024, Geologic map of the Big Hole Battlefield 7.5' quadrangle, southwestern Montana: Montana Bureau of Mines and Geology Geologic Map 97, 1 sheet, scale 1:24,000, https://doi.org/10.59691/QIYJ2150

Elliott, C.G., and Lonn, J.D., 2016, Geologic map of the Tash Peak 7.5' quadrangle, southwest Montana: Montana Bureau of Mines and Geology Open-File Report 678, 1 sheet, scale 1:24,000.

Elliott, C.G., and Lonn, J.D., 2021, Geologic map of the Foolhen Mountain 7.5' quadrangle, Beaverhead County, Montana: Montana Bureau of Mines and Geology Geologic Map 79, 1 sheet, scale 1:24,000.

Elliott, C.G., and Lonn, J.D., in prep., Geologic map of the Long Peak 7.5' quadrangle, southwestern Montana: Montana Bureau of Mines and Geology Geologic Map, 1 sheet, scale 1:24,000.

Evans, K.V., and Green, G.N., 2003, Geologic map of the Salmon National Forest and vicinity, east-central Idaho: U.S. Geological Survey Geologic Investigations Series Map I-2765, 2 sheets, scale 1:100,000, https://doi.org/10.3133/i2765

Flood, R.E., Jr., 1974, Structural geology of the upper Fishtrap Creek area, central Anaconda Range: Missoula, University of Montana, M.A. thesis, 71 p.

Foster, D.A., Mueller, P. A., Mogk, D.W., Wooden, J.L., and Vogl, J.J., 2006, Proterozoic evolution of the western margin of the Wyoming craton: Implications for the tectonic and magmatic evolution of the northern Rocky Mountains: Canadian Journal of Earth Sciences, v. 43, p. 1601–1619, https://doi.org/10.1139/E06-052

Foster, D.A., Grice Jr., W.C., and Kalakay, T.J., 2010, Extension of the Anaconda metamorphic core complex: $^{40}Ar/^{39}Ar$ thermochronology and implications for Eocene tectonics of the northern Rocky Mountains and the Boulder batholith: Lithosphere, v. 2, p. 232–246, https://doi.org/10.1130/L94.1

Foster, D.A., Mueller, P.A., Heatherington, A., Gifford, J.N., and Kalakay, T.J., 2012, Lu-Hf systematics of magmatic zircons reveal a Proterozoic crustal boundary under the Cretaceous Pioneer Batholith, Montana: Lithos v. 142–143, p. 216–225, https://doi.org/10.1016/j.lithos.2012.03.005

Fraser, G.D., and Waldrop, H.A., 1972, Geologic map of the Wise River quadrangle, Silver Bow and Beaverhead counties, Montana: U.S. Geological Survey Geologic Quadrangle Map GQ-988, 1 sheet, scale 1:24,000, https://doi.org/10.3133/gq988

Fritz, W.J., Sears, J.W., McDowell, R.J., and Wampler, J.M., 2007, Cenozoic volcanic rocks of southwestern Montana: Northwest Geology, v. 36, p. 91–110.

Geach, R.D., 1972, Mines and mineral deposits (except fuels), Beaverhead County, Montana: Montana Bureau of Mines and Geology Bulletin 85, 194 p., 3 sheets.

Gaschnig, R.M., Vervoort, J.D., Lewis, R.S., and Tikoff, B., 2011, Isotopic evolution of the Idaho batholith and Challis intrusive province, northern U.S. Cordillera: Journal of Petrology, v. 52, p. 2397–2429, https://doi.org/10.1093/petrology/egr050

Gobla, M.J., 2012, Montana Mineral Locality Index: Rocks and Minerals, v. 87, p. 208–240, https://doi.org/10.1080/00357529.2012.676825

Grice, W.C., Jr., 2006, Exhumation and cooling history of the middle Eocene Anaconda metamorphic core complex, western Montana: Gainesville, University of Florida, M.S. thesis, 261 p., available at https://ufdc.ufl.edu/ufe0015873/00001 [Accessed August 2025].

Gwinn, V.E., 1960, Cretaceous and Tertiary stratigraphy and structural geology of the Drummond area, western Montana: Princeton, Princeton University, Ph.D. dissertation, 153 p.

Gwinn, V.E., 1961, Geology of the Drummond area, central-western Montana: Montana Bureau of Mines and Geology Geologic Map 4, 1 sheet, scale 1:63,360.

Haney, E.M., 2008, Pressure-temperature evolution of metapelites within the Anaconda Metamorphic Core Complex, southwestern Montana: Missoula, University of Montana, M.S. thesis, 100 p.

Hanneman, D.L., 1984, Geologic map of the Wisdom quadrangle, Beaverhead County, Montana: U.S. Geological Survey Mineral Investigations Field Study Maps 1695, 1 sheet, scale 1:24,000, https://doi.org/10.3133/mf1695

Hanneman, D.L., 1987a, Geologic map of the Pintlar Lake quadrangle, Beaverhead and Deer Lodge counties, Montana: U.S. Geological Survey Mineral Investigations Field Study Maps 1931, 1 sheet, scale 1:24,000, https://doi.org/10.3133/mf1931

Hanneman, D. L., 1987b, Geologic map of the Pine Hill quadrangle, Beaverhead and Deer Lodge counties, Montana: U.S. Geological Survey Mineral Investigations Field Study Maps 1930, 1 sheet, scale 1:24,000, https://doi.org/10.3133/mf1930

Hanneman, D.L., and Nichols, R., 1981, Late Tertiary sedimentary rocks of the Big Hole Basin, south-

west Montana: Abstracts with Programs, Geological Society of America, v.13, no. 4, p. 199.

Howlett, C.J., Reynolds, A.N., and Laskowski, A.K., 2020, Geologic map of the northern half of the Pintler Lake 7.5' quadrangle and the southern half of the Warren Peak 7.5' quadrangle, southwestern Montana: Montana Bureau of Mines and Geology EDMAP portion of the National Geologic Mapping Program 13, 1 sheet, scale 1:24,000.

Howlett, C.J., Reynolds, A.N., and Laskowski, A.K., 2021, Magmatism and extension in the Anaconda metamorphic core complex of western Montana and relation to regional tectonics: Tectonics, v. 40, 31 p., https://doi.org/10.1029/2020TC006431

Hyndman, D.W., Bradley, R., and Rebal, D., 1977, Northeast-trending early Tertiary dike swarm in central Idaho and western Montana: Geological Society of America Abstracts with Programs, v. 9, no. 6, p. 734.

Janecke, S.U., 2007, Cenozoic extensional processes and tectonics in the northern Rocky Mountains: southwest Montana and eastern Idaho: Northwest Geology, v. 36, p. 111–132.

Lewis, S.E., 1993, Preliminary geologic map of the Lincoln Gulch quadrangle, southwestern Montana: Montana Bureau of Mines and Geology Open-File Report 272, 10 p., 1 sheet, scale 1:24,000.

Lidke, D.J., and Wallace, C.A., 1992, Rocks and structure of the north-central part of the Anaconda Range, Deer Lodge and Granite Counties, Montana: U.S. Geological Survey Bulletin 1993, 31 p., scale 1:24,000, https://doi.org/10.3133/b1993

Loen, J., and Pearson, R.C., 1989, Map showing locations of mines and prospects in the Dillon 1° x 2° quadrangle, Idaho and Montana: U.S. Geological Survey Miscellaneous Investigations Series Map I-1803-C, scale 1:250,000, https://doi.org/10.3133/i1803C

Lonn, J.D., 2015, Geologic map of the Maurice Mountain 7.5' quadrangle southwestern Montana: Montana Bureau of Mines and Geology Open-File Report 657, 1 sheet, scale 1:24,000.

Lonn, J.D., 2017, Geologic map of part of the Lick Creek 7.5' quadrangle, southwestern Montana: Montana Bureau of Mines and Geology Open File Report 690, scale 1:24,000.

Lonn, J.D., 2020, Geologic map of the south half of the Shaw Mountain 7.5' quadrangle, southwestern Montana: Montana Bureau of Mines and Geology Geologic Map 78, 1 sheet, scale 1:24,000.

Lonn, J.D., and Elliott, C.G., 2017, Geologic map of the Stine Mountain 7.5’ quadrangle, southwest Montana: Montana Bureau of Mines and Geology Geologic Map 69, 1 sheet, scale 1:24,000.

Lonn, J.D., and Johnson, L., 2010, Cretaceous structures and mineralization in the footwall of the Eocene Anaconda detachment fault, Montana: A field trip along Warm Springs Creek: Northwest Geology, v. 39, p. 57–68.

Lonn, J.D., and McDonald, C., 2004a, Geologic map of the Kelly Lake 7.5’ quadrangle, western Montana: Montana Bureau of Mines and Geology Open-File Report 500, 15 p., 1 sheet, scale 1:24,000.

Lonn, J.D., and McDonald, C., 2004b, Geologic map of the Dickie Hills 7.5’ quadrangle, southwest Montana: Montana Bureau of Mines and Geology Open-File Report 501, 14 p., 1 sheet, scale 1:24,000.

Lonn, J.D., Elliott, C.G., Lewis, R.S., Burmester, R.F., McFaddan, M.D., Stanford, L.R., and Jänecke, S.U., 2019, Geologic map of the Montana part of the Salmon 30’ x 60’ quadrangle, southwestern Montana: Montana Bureau of Mines and Geology Geologic Map 75, 28 p., 1 sheet, scale 1:100,000.

Lonn, J.D., and Mosolf, J.G., 2020, Field guide to the geology of the Sleeping Child metamorphic complex, southern Sapphire Mountains, western Montana: Northwest Geology, v. 49, p. 35–56.

Lonn, J.D., and Scarberry, K.C., 2022, Geologic map of the Odell Lake 7.5’ quadrangle, southwestern Montana: Montana Bureau of Mines and Geology Geologic Map 86, 1 sheet, scale 1:24,000.

Lonn, J.D., McDonald, C., Lewis, R.S., Kalakay, T.J., O’Neill, J.M., Berg, R.B., and Hargrave, P., 2003, Geologic map of the Philipsburg 30’ x 60’ quadrangle, western Montana: Montana Bureau of Mines and Geology Open-File Report 483, 1 sheet, scale 1:100,000.

Lonn, J.D., Burmester, R.F., Lewis, R.S., and McFaddan, M.D., 2020, The Mesoproterozoic Belt Supergroup, *in* Geology of Montana: Montana Bureau of Mines and Geology Special Publication

122, v 1: Geologic History, available at https://mbmg.mtech.edu/pdf/geologyvolume/Lonn_Belt-Final.pdf [Accessed August 2025].

Lonn, J.D., Burmester, R.F., and Lewis, R.S., 2023, The Mesoproterozoic Belt–Lemhi connection, western Montana and east-central Idaho: Northwest Geology, v. 52, p. 41–53.

Lonn, J.D., Elliott, C.G., Burmester, R.F., and Lewis, R.S., 2024, Geologic map of the Big Hole Pass 7.5' quadrangle, southwestern Montana and eastern Idaho: Montana Bureau of Mines and Geology Geologic Map 94, 1 sheet, scale 1:24,000, https://doi.org/10.59691/PBOA7465

Lopez, D.A., 1982, Reconnaissance geologic map of the Gibbonsville quadrangle, Lemhi County, Idaho and Beaverhead County, Montana: U.S. Geological Survey Miscellaneous Field Studies Map MF-1446, 1 sheet, scale 1:24,000, https://doi.org/10.3133/mf1446

Lopez, D.A., O'Neill, M., and Ruppel, E.T., 2005, Preliminary geologic map of the Big Hole Pass–Lost Trail Pass area, southwestern Montana: Montana Bureau of Mines and Geology Open-File Report 522, 8 p., 1 sheet, scale 1:48,000.

Lund, K., Rehn, W.M., and Holloway, C.D., 1983, Geologic map of the Blue Joint Wilderness Study Area, Ravalli County, Montana, and the Blue Joint Roadless Area, Lemhi County, Idaho: U.S. Geological Survey Miscellaneous Field Studies Map MF-1557-B, scale 1:50,000.

Marvin, R.F., Zen, E-An, Hammarstrom, J.M., and Mehnert, H.H., 1983, Cretaceous and Paleocene potassium-argon mineral ages of the northern Pioneer batholiths and nearby igneous rocks in southwest Montana: Isochron West, no. 38, p. 11–16.

McDonald, C., and Lonn, J.D., 2013, Revisions of Mesoproterozoic and Cambrian stratigraphy in the Pioneer and Highland Mountains, southwestern Montana, and resulting implications for the Paleogeography of the Belt Basin: Northwest Geology, v. 42, p. 93–102.

McDonald, C., Elliott, C.G., Vuke, S.M., Lonn, J.D., and Berg, R.B., 2012, Geologic map of the Butte South 30' x 60' quadrangle, southwestern Montana: Montana Bureau of Mines and Geology Open-File Report 622, 1 sheet, scale 1:100,000.

Messenger, J., 2016, Paragenesis and geochemistry of the Calvert tungsten skarn deposit, Pioneer Mountains, Montana: Butte, Montana Tech of the University of Montana, M.S. thesis, 99 p.

Messenger, J., and Gammons, C.H., 2017, Geology, fluid inclusions, and stable isotope study of the Calvert tungsten mine, Pioneer Mountains, Montana: Montana Bureau of Mines and Geology Open-File Report 685, p. 27–35.

Mosolf, J.G., and Kylander-Clark, A., 2023a, U-Pb geochronology data from rock samples collected in the Dillon, Hamilton, Philipsburg, Townsend, and Wisdom 30' x 60' quadrangles, western Montana, 2020–2021: Montana Bureau of Mines and Geology Analytical Dataset 3, https://doi.org/10.59691/FIIS4856

Mosolf, J.G., and Kylander-Clark, A., 2023b, U-Pb geochronology data from rock samples collected in the Dillon and Wisdom 30' x 60' quadrangles, western Montana, 2021–2022: Montana Bureau of Mines and Geology Analytical Dataset 4, https://doi.org/10.59691/CBJJ3933

Mosolf, J.G., and Kylander-Clark, A., in review, LA-ICPMS U-Pb geochronology data from rock samples collected in the Butte North, Dillon, Hamilton, Polson, and Wisdom 30' x 60' quadrangles, western Montana, 2019–2020: Montana Bureau of Mines and Geology Analytical Dataset.

Mosolf, J.G., Brennan, D.T., and Kylander-Clark, A., 2023a, LA-ICPMS U-Pb geochronology data from rock samples collected in the Dillon, Ennis, Gardiner, Hamilton, Hebgen Lake, and Wisdom 30' x 60' quadrangles, western Montana, 2022–2023: Montana Bureau of Mines and Geology Analytical Dataset 5, https://doi.org/10.59691/ZQRI9918

Mosolf, J.G., Hanson, A.E.H., McDonald, C., Parker, S., and Scarberry, K., 2023b, Major oxide and trace element analyses of rock samples collected in the Dillon and Wisdom 30' x 60' quadrangles, southwest Montana: Montana Bureau of Mines and Geology Analytical Dataset 1, https://doi.org/10.59691/TEOF5831

Mosolf, J., Lewis, R.S., and Burmester, R.F., 2023c, Field guide to Challis volcanic group in the Agency Creek and Lemhi Pass areas, Idaho and Montana: Northwest Geology, v. 52, p. 219–231.

Murphy, J.G., Foster, D.A., Kalakay, T.J., John, B.E., and Hamilton, M., 2002, U–Pb zircon geochronology of the Eastern Pioneer igneous complex, SW Montana: Magmatism in the foreland of the Cordilleran fold and thrust belt: Northwest Geology, v. 31, p. 1–11.

Mutch, T.A., 1960, Geology of the northeast flank of the Flint Creek Range, Montana: Princeton, Princeton University, Ph.D. dissertation, 159 p.

Mutch, T.A., 1961, Geology of the northeast flank of the Flint Creek Range, western Montana: Montana Bureau of Mines and Geology Geologic Map 5, 1 sheet, scale 1:63,360.

Neal, B.A., Burrell, W.B., Laskowski, A.K., and Lonn, J.D., 2023a, Geologic map of the Carpp Ridge 7.5′ quadrangle, southwestern Montana: Montana Bureau of Mines and Geology EDMAP portion of the National Geologic Mapping Program 15, 1 sheet, scale 1:24,000.

Neal, B.A., Laskowski, A.K., Lonn, J.D., and Burrell, W.B., 2023b, Kilometer-scale recumbent folding, tectonic attenuation, and rotational shear in the western Anaconda Range, southwestern Montana, USA: Geosphere, v. 19, no. 6, p. 1616–1639, https://doi.org/10.1130/GES02595.1

O'Neill, J.M., Lonn, J.D., Lageson, D.R., and Kunk, M.J., 2004, Early Tertiary Anaconda Metamorphic Core Complex, southwestern Montana: Canadian Journal of Earth Sciences, v. 41, p. 63–72, https://doi.org/10.1139/E03-086

Pearson, R.C., and Zen, E-an, 1985, Geologic map of the Eastern Pioneer Mountains, Beaverhead County, Montana: U.S. Geological Survey Miscellaneous Field Studies Map MF-1806-A, https://doi.org/10.3133/mf1806A

Roe, W.P., 2010, Tertiary sediments of the Big Hole Valley and Pioneer Mountains, southwestern Montana: Age, provenance, and tectonic implications: Missoula, University of Montana, M.S. thesis, 120 p., available at https://scholarworks.umt.edu/etd/1318 [Accessed August 2025].

Ruppel, E.T., and Lopez, D.A., 1984, The thrust belt in southwest Montana and east-central Idaho: U.S. Geological Survey Professional Paper 1278, 41 p., https://doi.org/10.3133/pp1278

Ruppel, E.T., O'Neill, J.M., and Lopez, D.A., 1993, Geologic map of the Dillon 1° x 2° quadrangle, Idaho and Montana: U.S. Geological Survey Miscellaneous Investigations Series Map I-1803-H, scale 1:250,000, https://doi.org/10.3133/i1803H

Scarberry, K.C., Elliott, C.G., and Yakovlev, P.V., 2019, Geologic map of the Butte North 30' x 60' quadrangle, southwest Montana: Montana Bureau of Mines and Geology Open-File Report 715, 30 p., 1 sheet, scale 1:100,000.

Schwartz, R.K., Schwartz, T.M., and Elliott, C.G., in review, Paleogene tectonic, landscape, and basin evolution in the Missouri River Headwater and Anaconda Detachment Region of the Basin and Range Province in southwestern Montana. Montana Bureau of Mines and Geology Memoir.

Sears, J.W., Hendrix, M.S., Thomas, R.C., and Fritz, W.J., 2009, Stratigraphic record of the Yellowstone hotspot track, Neogene Sixmile Creek Formation grabens, southwest Montana: Journal of Volcanology and Geothermal Research, v. 188, p. 250–259, https://doi.org/10.1016/j.jvolgeores.2009.08.017

Simonsen, S.W., 1997, $^{40}Ar/^{39}Ar$ ages of Eocene dikes and the age of extension in a Tertiary magmatic arc, Idaho and Montana: MS thesis, University of Montana, M.S. thesis, 121 p., available at https://scholarworks.umt.edu/etd/4671 [Accessed August 2025].

Snee, L.W., 1982, Emplacement and cooling of the Pioneer batholith, southwestern Montana: Columbus, Ohio State University, Ph.D. dissertation, 320 p.

Stewart, D.E., Lewis, R.S., Lonn, J.D., Salazar, R., Burmester, R.F., and Elliott, C.E., 2025, Geologic map of the Lost Trail Pass quadrangle, Lemhi County, Idaho, and Beaverhead and Ravalli Counties, Montana: Montana Bureau of Mines and Geology Geologic Map 102, 1 sheet, scale 1:24,000, https://doi.org/10.59691/LQQA5158

Stewart, E.D., Steele, E.D., Stewart, D.E., and Link, P.K., 2014, Geologic map of the Gibsonville, Shewag Lake, and Allan Mountain quadrangles, and parts of the Lost Trail Pass and Big Hole Pass quadrangles: Idaho Geological Survey Technical Report 14-2, scale 1:40,000.

Toth, M.I., 1983, Reconnaissance geologic map of the Selway–Bitterroot Wilderness, Idaho County, Idaho, and Missoula and Ravalli Counties, Mon-

tana: U.S. Geological Survey Miscellaneous Field Studies Map MF-1495B, scale 1:125,000, https://doi.org/10.3133/mf1495B

Toth, M.I., 1987, Petrology and origin of the Bitterroot lobe of the Idaho batholith, *in* Vallier, T.L., and Brooks, H.C., eds., Geology of the Blue Mountains region of Oregon, Idaho, and Washington: U.S. Geological Survey Professional Paper 1436, p. 9–35.

Truckle, D.M., 1988, Geology of the Calvert Hill area, Beaverhead County, Montana: Butte, Montana Tech, M.S. thesis, 94 p., map scale 1:24,000.

Van Wagoner, N., and Ootes, L., 2024, Early Eocene volcanism in the Cordilleran Orogen of northwestern North America and its tectonic implications: Geological Society of America Abstracts with Programs, v. 56, no. 4, https://doi.org/10.1130/abs/2024CD-399913

Vuke, S.M., 2019, The Eocene through early Miocene sedimentary record in western Montana, *in* MBMG Special Publication 122: Geology of Montana, v. 1, available at https://www.mbmg.mtech.edu/pubs/GeologyofMontana/ [Accessed August 2025].

Walker, D.D., 1963, Tungsten resources of western Montana: U.S. Bureau of Mines Report of Investigations 6334, 60 p.

Wallace, C.A., Lidke, D.J., Elliott, J.E., Desmarais, N.R., Obradovich, J.D., Lopez, D.A., Zarske, S.E., Heise, B.A., Blaskowski, M.J., and Loen, J.S., 1992, Geologic map of the Anaconda–Pintlar Wilderness and contiguous roadless area, Granite, Deer Lodge, Beaverhead, and Ravalli counties, western Montana: U.S. Geological Survey Miscellaneous Field Studies Map 1633-C, 1 sheet, scale 1:50,000, https://doi.org/10.3133/mf1633C

Wiswall, C.G., 1976, Structural styles of the southern boundary of the sapphire tectonic block Anaconda–Pintlar Wilderness Area, Montana: Missoula, University of Montana, M.S. thesis, 62 p., scale 1:48,000, available at https://scholarworks.umt.edu/etd/7118 [Accessed August 2025].

Worthington, J.E., 2007, Porphyry and other molybdenum deposits of Idaho and Montana: Idaho Geological Survey Technical Report 07-3, 22 p.

Zen, E-An, 1988, Bedrock geology of the Vipond Park 15', Stine Mountain 7.5', and Maurice Mountain 7.5' quadrangles, Pioneer Mountains, Beaverhead County, Montana: U.S. Geological Survey Bulletin 1625, 49 p., scale 1:62,500, https://doi.org/10.3133/b1625

Zimbelman, D.R., 1984, Geology of the Polaris 1SE quadrangle, Beaverhead County, Montana: Boulder, University of Colorado, M.S. thesis, 154 p.